Neuroscience
2013

SHORT COURSE I

Chemo and Optogenetics: Light and Chemical Control of Neurons

Organized by Luis de Lecea, PhD

SfN Society for Neuroscience

Short Course I

Chemo and Optogenetics: Light and Chemical Control of Neurons

Organized by Luis de Lecea, PhD

Society for Neuroscience

Please cite articles using the model:
[AUTHOR'S LAST NAME, AUTHOR'S FIRST & MIDDLE INITIALS] (2013)
[CHAPTER TITLE] In: Chemo and Optogenetics: Light and Chemical Control of Neurons.
(de Lecea, L, ed) pp. [xx-xx].
Washington, DC: Society for Neuroscience.

All articles and their graphics are under the copyright of their respective authors.

Cover graphics and design © 2013 Society for Neuroscience.

Neuroscience
2013

SHORT COURSE #1

Chemo and Optogenetics: Light and Chemical Control of Neurons

Organized by: Luis de Lecea, PhD
Friday, November 8
8:30 a.m. – 6:30 p.m. | San Diego | The San Diego Convention Center | Room: 6B

TIME	AGENDA TOPICS	SPEAKER
7:30 – 8:00 a.m.	**CHECK-IN**	
8:00 – 8:10 a.m.	Opening remarks	Luis de Lecea, PhD *Stanford University*
8:10 – 8:55 a.m.	Optogenetics: tools and applications	Karl Deisseroth, MD, PhD *Stanford University*
8:55 – 9:40 a.m.	Chemical actuators of neuronal actvity	Bryan Roth, MD, PhD *University of North Carolina*
9:40 – 9:55 a.m.	**MORNING BREAK**	
9:55 – 10:40 a.m.	ITBD	Ilana Witten, PhD *Princeton University*
10:40 – 11:25 a.m.	Deconstruction of brain reward circuits	Garret Stuber, PhD *University of North Carolina*
11:25 a.m. – 12:10 p.m.	Decoding the brain serotonergic system: functional probing with chemogenetics	Susan Dymecki, PhD *Harvard Medical School*
12:10 – 1:10 p.m.	**LUNCH: ROOM 33ABC**	
1:10 – 1:55 p.m.	Wireless optogenetics	Michael Bruchas, PhD *Washington University St Louis*
1:55 – 2:40 p.m.	Genetically encoded biosensors of neuronal activity	Thomas Knöpfel, MD, PhD *Imperial College London*
2:40 – 3:40 p.m.	**SUMMARY, DISCUSSION, BREAKOUT GUIDE**	
3:40 – 4:00 p.m.	**AFTERNOON BREAK**	

AFTERNOON BREAKOUT SESSIONS

Participants select one discussion group at 4:00 p.m. and one at 5:00 p.m.

TIME	THEME	ROOM
4:00 – 5:00 p.m.	**BREAKOUT SESSIONS**	
	GROUP 1 – Optogenetic applications Luis de Lecea, PhD, Garret Stuber, PhD, Ilana Witten, PhD	33A
	GROUP 2 – Chemo-pharmacogenetics Susan Dymecki, PhD, Bryan Roth, MD, PhD	33B
	GROUP 3 – New technologies associated with optogenetics Michael Bruchas, PhD, Karl Deisseroth, MD, PhD, Thomas Knöpfel, MD, PhD	33C
5:00 – 6:00 p.m.	**REPEAT SESSIONS ABOVE. SELECT A SECOND DISCUSSION GROUP.**	

SFN Society for Neuroscience

Table of Contents

Introduction

The ability to manipulate the activity of genetically defined neurons has revolutionized neuroscience. It is now possible to interrogate the function of neuronal circuits in behavior with unprecedented specificity and temporal precision.

Optogenetics is based on targeting light-sensitive opsin molecules in specific neuronal populations to enable excitation or inhibition of neuronal circuits. In the past few years, optogenetic techniques have been used to uncover new components of sensory, motor, and limbic processing. Several recent developments in the field are leading to important breakthroughs. For example, the recent determination of the crystal structure of channelrhodopsin-2 will allow the design of new optogenetic probes with different current properties and activation spectra. Also, new devices to increase the efficiency of light delivery in the brain are being developed. Further, the combination of genetically encoded optical sensors of neuronal activity (e.g., GCaMP6) with optogenetic actuators is leading to all-optical control and functional interrogation of neuronal circuits during complex behavioral tasks.

The use of modified designer receptors, or DREADDs (designer receptors exclusively activated by designer drug), is an essentially different, complementary approach to manipulating cell-type-specific neuronal activity. When expressed in neurons, DREADDs do not bind endogenous ligands but are sensitive to the orally available ligand clozapine-*N*-oxide (CNO), which is otherwise pharmacologically inert. DREADDs are particularly attractive for studying the function of modulators with longer time scales.

This short course will highlight advances in our understanding of CNS function enabled by optogenetic and pharmacogenetic methods. It will also emphasize the complexities of functional analysis of neuronal circuits.

Current Challenges in Optogenetics

Kelly A. Zalocusky, Lief E. Fenno, and Karl Deisseroth, MD, PhD

Howard Hughes Medical Institute
Departments of Bioengineering and Psychiatry
Stanford University
Stanford, California

© 2013 Deisseroth

NOTES

Introduction

Studying intact systems with simultaneous local precision and global scope is a fundamental challenge of biology, and part of the solution may be found in optogenetics. This field combines genetic and optical methods to achieve gain or loss of function of temporally defined events in specific cells embedded within intact living tissue or organisms. Such precise causal control within the functioning intact system can be achieved by introducing genes that confer to cells both light-detection capability and specific effector function. For example, microbial opsin genes can be expressed in neurons to mediate millisecond precision and reliable control of action potential firing in response to light pulses (Boyden et al., 2005; Ishizuka et al., 2006; Yizhar et al., 2011). Indeed, this approach has now been used to control neuronal activity in a wide range of animals and systems, yielding insights into fundamental aspects of physiology as well as into dysfunction and possible treatments for pathological states (Fenno and Deisseroth, 2013). Many other strategies for optical control (besides the microbial opsin gene approach) may be applied as well (Möglich and Moffat, 2007; Wu et al., 2009; Airan et al., 2009; Stierl et al., 2011). Yet despite the field's diversity of approaches, rapid growth, and wide scope of applications, fundamental challenges remain to be addressed in basic technology development. In this chapter, we review these challenges as well as the opportunities at hand, and aspects of the figures and text build on the findings of recent reviews (Yizhar et al., 2011; Zhang et al., 2011; Fenno and Deisseroth, 2013; Zalocusky and Deisseroth, 2013).

Background: Current Functionality of Tools

Diverse and elegant mechanisms have evolved to enable organisms to harvest light for survival functions (Fig. 1). For example, opsin genes encode 7-transmembrane (7-TM) proteins that, when bound to the small organic chromophore all-*trans* retinal, constitute light-sensitive rhodopsins, which are found across all kingdoms of life. Many prokaryotes employ these proteins to control proton gradients and to maintain membrane potential and ionic homeostasis, and many motile microorganisms have evolved opsin-based photoreceptors to modulate flagellar motors and thereby direct phototaxis toward environments with optimal light intensities for photosynthesis. Owing to their structural simplicity (both light-sensing and effector domains are encoded within a single gene) and fast kinetics, microbial rhodopsins can be treated as precise and modular photosensitization components for introduction into non-light-sensitive cells to enable rapid optical control of specific cellular processes (Yizhar et al., 2011). Alternatively, the light receptor can be a small organic molecule that is introduced into the biological system, with or without a designed binding protein as effector. Many other nonopsin classes of naturally occurring proteins have been explored as well. These include flavin chromophore–utilizing light-activated enzymes, such as adenylyl cyclases, as well as engineered systems in which light-sensation modules become physically linked to effector modules (Möglich and Moffat, 2007; Airan et al., 2009; Wu et al., 2009; Stierl et al., 2011).

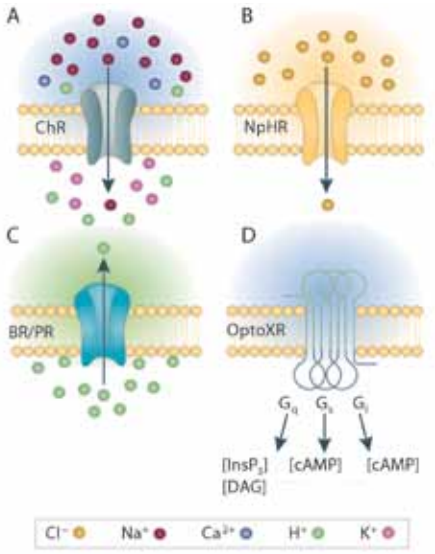

Figure 1. Single-component optogenetic tool categories. Four major classes of opsin commonly used in optogenetics experiments, each encompassing light sensation and effector function within a single gene, include: (1) ChRs, which are light-activated cation channels that give rise to inward (excitatory) currents under physiological conditions; (2) halorhodopsins (NpHR shown), which are inhibitory (outward-current) chloride pumps; (3) bacteriorhodopsins and proteorhodopsins (BR/PR), proton pumps that tend to be inhibitory and include archaerhodopsins; and (4) OptoXRs, which modulate secondary messenger-signaling pathways. Adapted from Zalocusky and Deisseroth (2013), their Figure 1. © Versita Sp. z o.o.

The experimental potential of optogenetics has triggered a surge of genome prospecting and molecular engineering to expand the repertoire of tools and generate new functionality. This expansion, in turn, has catalyzed further mechanistic studies of microbial proteins (Zhang et al., 2011). High-resolution crystal structures are now available for most of the major photoreceptor modules, including most recently, channelrhodopsin (ChR) (Kato et al., 2012). This information has been important not only for enhancing understanding of mechanism but also for guiding optogenetics in the generation of variants with novel function related to spectrum, selectivity, and kinetics. For example, ChR variants

© 2013 Deisseroth

NOTES

have been engineered with shorter or longer open-state lifetimes, shifted absorption spectra, reduced desensitization, increased expression, and increased photocurrent magnitude (Yizhar et al., 2011; Mattis et al., 2012). Likewise, high-resolution crystal–structural insights have been used to help guide the assembly of light-sensitive modules, together with effector modules, into artificial proteins. In this way, parallel information streams have been created that are capable of carrying optogenetic control signals for modulation purposes (Möglich and Moffat, 2007).

This diversity of optogenetic tool function will be important for making significant headway in our understanding both of normal brain function and of dysfunctional processes in neuropsychiatric disease. For example, many disease states arise in part from impaired interaction of multiple distinct cell or projection types. This etiology points to the experimental value of achieving multicolor excitation and multicolor inhibition optogenetically within the same living mammalian brain for neuropsychiatry research. It is encouraging that optogenetic interventions have now built a secure foothold for the study of both normal function and brain disease states. Nevertheless, major areas of optogenetic tool advancement are required in the future, as detailed next.

Unsolved Problems and Open Questions in Technology

Addressing the technological challenges that follow, all squarely in the domain of modern neuroscience, will help provide experimental leverage that may lead to key insights into neural circuit function and dysfunction. Such insights would be difficult or impossible to establish by other means.

Cell biology

One group of technological challenges to be addressed by optogenetics lies within the natural domain of metazoan biology. The development of guided subcellular trafficking will be an important step, and membrane trafficking strategies have already improved the expression of opsins at the membrane (Gradinaru et al., 2008). Further exploration in this area may produce targeting strategies that will allow selective optogenetic tool expression in subcellular compartments such as dendrites, somata, or axon terminals. Indeed, while efforts have been made in this regard, achieving truly robust (near 100%) exclusion of heterologously expressed optogenetic proteins from axons would prevent the undesired optical drive of axons of passage during illumination of a transduced brain region. The expression of optogenetic tools in axons is one of the most useful features of this approach in that it allows "projection targeting"–based recruitment of cells defined only by selective illumination and projection pattern (Yizhar et al., 2011; Fenno et al., 2013; Fenno and Deisseroth, 2013; Zalocusky and Deisseroth, 2013). However, this effect also confounds certain kinds of functional mapping procedures that employ optogenetics.

Optics

It also would be valuable to develop a robust and versatile optical (nonpharmacological) strategy. This would prevent (when desired) the propagation of optogenetically elicited action potentials in the antidromic direction or along axon collaterals during projection-targeting experiments. Although this antidromic drive is sometimes desired, in other cases, it is not, i.e., when the experimenter seeks to allow generalizable selective excitation only of spatially defined projections and does not wish to take advantage of the existing capability to recruit cells defined by projection (Yizhar et al., 2011).

Behavior

Improved high-speed volumetric (three-dimensional) light delivery strategies with single-cell resolution would be of great value, in that populations of cells (even within intact mammalian brain tissue) could be recruited optogenetically with any required extent of synchrony or asynchrony. For example, optogenetics applications to questions of mammalian circuit dynamics and behavior *in vivo* have typically involved synchronous optogenetic control of entire genetically targeted cell populations over millimeter-scale spatial domains. Examples include studies of sleep–wake transitions, parkinsonian circuitry, gamma rhythms, feeding behavior, olfaction, aggression, and memory consolidation. Yet methods for guiding spatial delivery of multiple wavelengths of light excitation in three-dimensional volumes could yield much improved precision and complexity in optogenetic modulation. These methods would take the next step beyond the single-photon, guided-light strategies that have already been used, even in mammalian tissue, for applications such as highly refined optogenetic circuit mapping and dissection of anxiety circuitry. Optogenetic two-photon illumination could provide a distinct means of manipulating single or multiple genetically and spatially targeted cells with high temporal resolution over sustained intervals and within intact tissue volumes. This technique would then be able to delineate and define components that work in concert to generate circuit dynamics or behavior.

© 2013 Deisseroth

NOTES

One pioneering two-photon study was able to overcome the low, single-channel conductance of ChR2 and to produce action potentials in cultured neurons using complex scan patterns in order to open sufficient channels on individual neurons. Two-photon optogenetic manipulation of spatially and genetically defined cells within intact tissue volumes with simpler (standard) raster scanning would further broaden the reach of this approach to many laboratories worldwide. Two other reports of neuron activation in slice preparations with optogenetics relied on elegant hardware innovations and larger focal spots of laser illumination to overcome the modest conductance of individual channels. Other nonscanning methods, such as spatial light modulators (SLMs) and light-field microscopy, could allow myriad opportunities to probe the temporal mechanisms by which population codes are set up and employed in neural circuit function. Two recent reports have made headway in developing two-photon raster scanning and SLM-based methods for versatile optogenetic control in intact tissue or *in vivo* in mammals (Packer et al., 2012; Prakash et al., 2012).

Extension to other species and cell types

Robust extension of optogenetic tool-targeting strategies to non–genetically tractable species or cell types will be enormously helpful. The generation of Cre-driver rats has been important, and projection targeting provides an independent step forward.

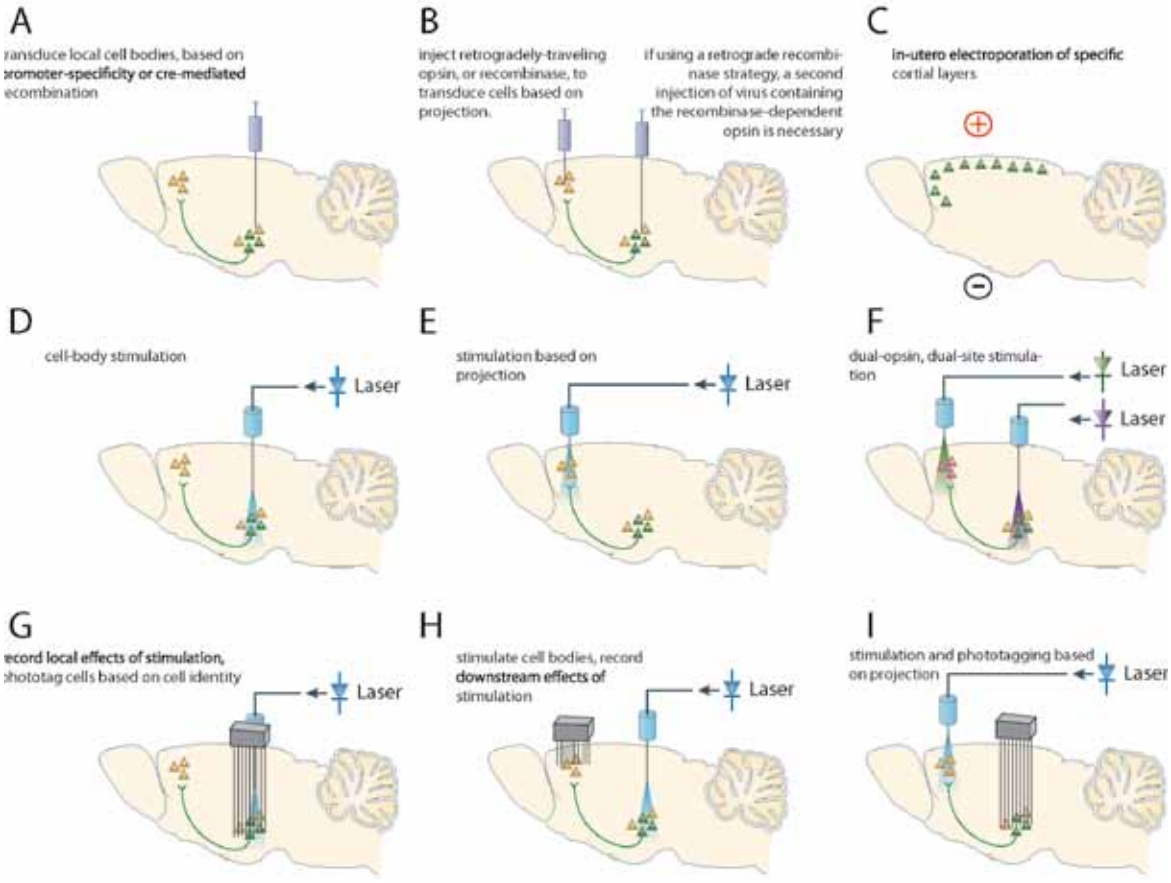

Figure 2. Optogenetic targeting and experimental design suitable for any vertebrate species, including mouse, rat, and primate. Panels *A–C* illustrate strategies for transducing the cell population of interest with an opsin. These include *A,* transduction of cell bodies via viral injection, *B,* single- or dual-virus retrograde strategies for projection-specific opsin expression, and *C, in utero* electroporation for cortical-layer-specific expression. Panels *D–F* illustrate possible configurations for optical stimulation, including *D,* illumination at the site of transduced cell bodies, *E*, illumination of downstream projections, and *F,* illuminating multiple distinct populations of cells at the same or different locations, which can express opsins sensitive to different wavelengths of light. Panels *G–I* illustrate combinations of electrical recording with optical stimulation. Possible configurations include *G,* recording at the site of optical stimulation, *H,* recording downstream of optical stimulation, and *I,* recording at transduced cell bodies while stimulating downstream projections. Adapted from Fenno and Deisseroth (2013) and Zalocusky and Deisseroth (2013), their Figure 2.

© 2013 Deisseroth

NOTES

But improved intersectional targeting strategies will also be crucial since few relevant cell types can be specified by only a single descriptor, e.g., cell body location, projection target, or activity of one promoter/enhancer region. Thus, designing and validating optogenetic tool-carrying viruses or other vectors that depend on multiple recombinases (for example, with Boolean and or other logical gates) will be essential. Also, developing improved methods to selectively exclude optogenetic tool expression in cells with a given genetic identity will be useful.

Wiring-based (connectomic) strategies

Finally, true retrograde and anterograde wiring-based strategies (i.e., targeting cells that project to a particular region, or cells that receive projections from a particular region) would greatly enhance the flexibility of optogenetic control, both in mice and in other species. Although such strategies exist, they are not always robust or well tolerated (Fenno and Deisseroth, 2013; Zalocusky and Deisseroth, 2013) (Fig. 2).

It would be immensely valuable to develop methods to rapidly and efficiently extract brainwide wiring (connectomic) patterns, or at least projection patterns, from optogenetically driven cells that had been shown to have a known and quantifiable impact on behavior in the very same animal. Further, it would be of great value to rapidly and efficiently extract the brainwide elicited-activity patterns arising from optogenetic control of a targeted population. This can be achieved to some extent with optogenetic functional magnetic resonance imaging (ofMRI), an optogenetic method that enables unbiased global assessment of the neural circuits upstream and downstream of focal stimulation. However, fMRI methods in general suffer from poor spatial and temporal resolution. Overall, improving the integration of optogenetic control with readouts—whether behavioral, electrophysiological, or imaging—will be important. Moreover, closing the loop so that neural activity or behavioral readouts can feed back and control the inputs played in via optogenetics will be of great interest, as will the development of computational methods to begin "reverse engineering" the studied circuitry by identifying the underlying transformations of information carried out in the tissue.

Unsolved Problems and Open Questions in Genomics and Biophysics

Another group of technological challenges to be addressed by optogenetics falls more into the natural domain of microbial biologists and protein biophysicists. (Of course, many laboratories and investigators span the metazoan and the microbial realms.)

Engineering better tools

The ongoing identification of additional genomically identified tools (e.g., via databases searches, broad-based next-generation sequencing efforts, and ecological genome mining) is expected to profoundly improve our ability to perturb and understand biological systems (Zhang et al., 2011; Mattis et al., 2012). Many thousands of new light-sensitive modules will be accessible in this way. For example, even though known opsins already span most of the visual spectrum and a broad kinetic space, it is very likely that new kinds of light sensitivity, kinetic properties, and even ion selectivity will emerge. One important goal is to move toward the infrared,

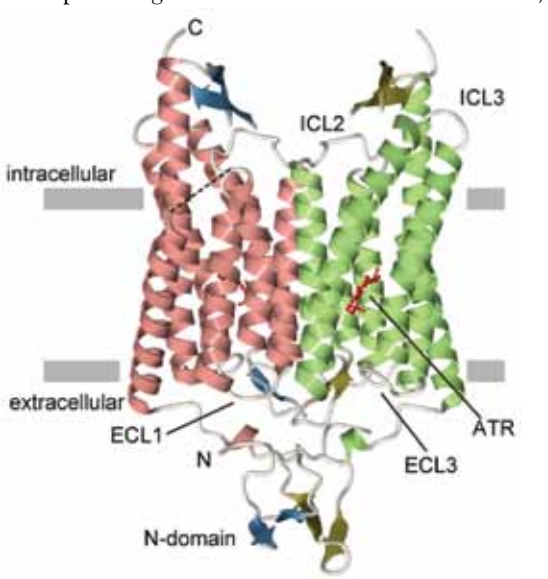

Figure 3. Channelrhodopsin crystal structure. This structure is of C1C2, a chimera between ChR1 and ChR2, consisting of the *N*-domain, with the 7-transmembrane helices connected by extracellular loops (ECLs) and intracellular loops (ICLs), and a truncated *C*-domain. All-*trans*-retinal (ATR) is red. This high-resolution structure includes description of the environment around the retinal-binding pocket, which will enable the optimized design of red- and blue-shifted ChR variants. In addition, the structure of the cation-conducting pathway may facilitate construction of ChR variants with improved photocurrents, photosensitivity, cation selectivity, and kinetics. Already, structure-guided mutagenesis has resulted in some degree of K^+ selectivity, which could be useful for suppressing neural activity. Further structural studies, including determination of crystal structures in intermediate states, are clearly needed that will help enable the principled design of ChR variants with new properties. These, in turn, will both accelerate the applications of optogenetics to intact-systems biology and further the basic mechanistic understanding of these remarkable photoreceptor proteins. Adapted with permission from Kato et al. (2012). © Nature Publishing Group.

© 2013 Deisseroth

NOTES

which will (1) achieve deeper light penetration at a given irradiance value; (2) reduce scattering (for improved resolution); and (3) provide an additional control channel. Infrared actuation has already been achieved for certain nonopsin-based optogenetic approaches, but it may encounter physics-based limitations for retinal-based photoreceptors.

Engineering these known or new tools for narrowed (as well as shifted) action spectra would enable cleaner separation of control channels. For example, engineering blue-shifted hyperpolarizing opsins with narrower activation wavelength spectra could ultimately allow researchers to enhance combinatorial neuronal inhibition experiments within scattering mammalian tissue volumes. Although action-spectrum peaks for existing tools span the visible spectrum and beyond, the broad shoulders of relevant action spectra might prevent the use of more than 2–3 channels of control at once, unless spectra can be narrowed. Such efforts might involve mutations that prevent access of the photocycle to specific states or intermediates that have shifted absorbance properties. This class of engineering will be facilitated by structure-based insights into the photocycle. For example, to understand the ChR photocycle in more detail, it will be necessary to undertake studies beyond the current closed-state structure ones (Kato et al., 2012; Fig. 3) and including open and intermediate photocycle states. These efforts may also lead to the generation of mutants with novel kinetic properties (Stehfest and Hegemann, 2010).

Light-sensitive pumps and channels

Engineering optogenetic light sensors for higher quantum efficiency, greater light sensitivity, and/or increased biological effect (e.g., current) elicited per protein molecule would be of substantial value because it would enable the use of lower irradiances for targeting a given tissue volume or depth. Also, lower irradiance might be important for minimizing photo damage, heating, or power use/deposition constraints (Lin et al., 2009; Yizhar et al., 2011; Mattis et al., 2012). Although, for opsins, many orders of magnitude of increased light sensitivity can be achieved using the bistable or step-function opsin (SFO) approach, this comes at a kinetic cost: slowing down the deactivation after light-off (Stehfest and Hegemann, 2010).

Developing a potent electrically inhibitory optogenetic channel (rather than a pump) would be of immense value. Current hyperpolarizing tools are pumps rather than channels, and therefore do not provide shunting or input-resistance changes (also, they can move only one ion per photon). As a result, these optogenetic tools are not nearly as effective as the channels or native inhibitory receptors—especially in projection-targeting experiments whose goal is to intercept action potentials in axons. Developing a potent electrically inhibitory optogenetic channel would also rapidly enable the generation of a hyperpolarizing SFO or bistable optogenetic tool (Stehfest and Hegemann, 2010; Yizhar et al., 2011; Fenno et al., 2013). This tool would enable sustained inhibition of neurons without requiring constant illumination. New structural knowledge of the ChR cation-conducting pathway and pore vestibules may facilitate construction of ChR variants with potassium selectivity for this purpose, as well as improved photocurrents, light sensitivity, and kinetic properties (Kato et al., 2012).

Controlling for opsin effects

Elsewhere, we have cautioned that powerful and prolonged light delivery can cause heating effects that could, in principle, alter neural activity even in nonexpressing cells. We have provided quantitative estimates of the magnitude of this effect (Yizhar et al., 2011). This potential confound can be addressed by maintaining moderate-intensity or pulsed-light protocols and by including experimental cohorts in which no opsin is expressed but all other manipulations are performed in the target animals (e.g., surgery, viral transduction, hardware implantation, and light delivery) (Yizhar et al., 2011). Similar controls are useful for identifying and/or correcting for confounds linked to any perception of the light by the animal's sensory systems. Moreover, overexpression of any foreign protein could cause altered structure, function, or survival of host cells, and opsins are no exception to this rule.

Despite these caveats, optogenetic methods do intrinsically provide a powerful means for controlling for such effects by allowing light-on and light-off assessment of physiology or behavior in each experimental subject. This technique ensures normal baseline behavior in the same animal at virtually the same time. Further, overexpression of control proteins in parallel experimental animals allows the experimenter to ensure that light effects are not being observed only because the animal or tissue is in an unusual state imposed by opsin expression independent of optical activation. Fluorescent proteins (XFPs) are most often employed as this control protein, since opsins are often expressed as XFP fusions; ongoing work is focusing on developing

© 2013 Deisseroth

NOTES

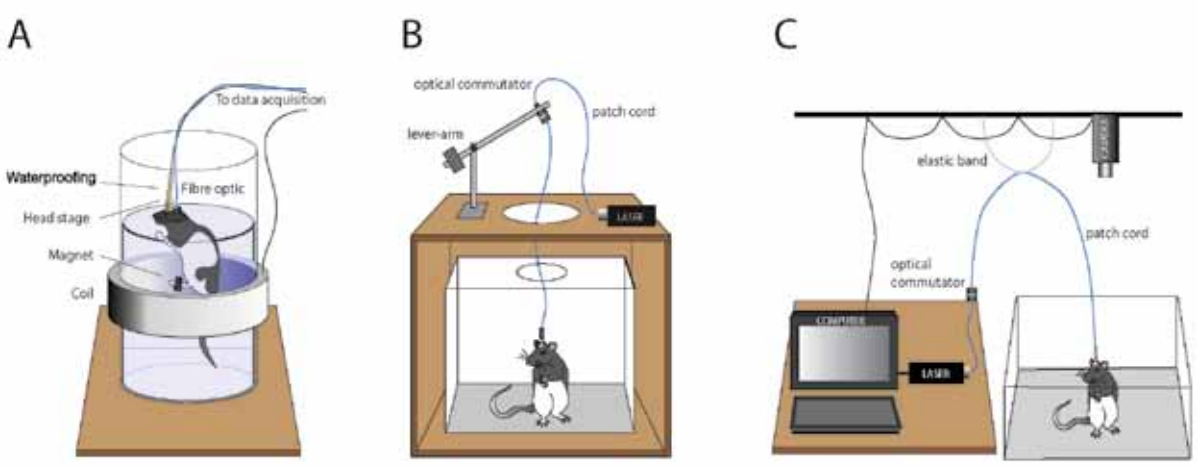

Figure 4. Integrating optogenetics with behavior. Diverse behavioral rigs can be outfitted for optogenetic experimentation. *A,* The forced swim test has been automated with magnetic induction–based detection of kicks combined with optogenetic stimulation and electrical recording. *B,* Operant behavior can also be combined with optogenetics. The chamber itself is modified to accommodate the entry of fiber optics and recording wires, and the stimulation/recording assembly is kept out of reach of the rodent with a counterweighted lever arm. *C,* Optogenetic manipulations can also be combined with behavior in open fields or large mazes. In these experiments, an elastic band, rather than a lever arm, is used to support stimulation/recording equipment. Video recording, combined with custom or commercially available software, can be used to synchronize optical stimulation with behavior. Adapted from Zalocusky and Deisseroth (2013), their Figure 4. © Versita Sp. z o.o.

photocurrent-null opsins for improved experimental control purposes. Such truly "dead" optogenetic tool mutants, having expression and targeting properties comparable with active tools but with no light-induced effector function, would be useful as controls to ensure that effects seen are specifically the result of optical recruitment of opsins in targeted cells. However, it will be important to ensure that the photocurrents are truly zero even under high membrane expression levels *in vivo*. Knowledge of pore structure (and pump mechanisms) may facilitate the generation of such tools (Kato et al., 2012).

Optically recruited biochemical signaling

In addition to light-sensitive pumps and channels, continued expansion of optically recruited biochemical signaling will be a significant development. Increasing attention should be given to strategies for recruiting modular and easily programmable signaling pathways, improving specificity, expanding spectral responsivity bands, and adapting to additional classes of native chromophores (e.g., flavins and biliverdins) (Stierl et al., 2011). We expect to see the OptoXR family of light-activated 7-TM neurotransmitter/neuromodulator receptors adding novel tools based on chimeras between vertebrate rhodopsins and both well-known and orphan G-protein coupled receptors (GPCRs) (Airan et al., 2009). In addition, light-sensitive domains are being added to an increasing number of receptors and even intracellular signaling proteins. In this way, optogenetics promises to expand to occupy the full breadth of cell signaling, far beyond the study of neural activity (Wu et al., 2009).

Conclusion

The discovery and engineering of new and improved classes of optogenetic control will come from continued microbial and biophysical investigations into ecological diversity, high-resolution structures, photocycle properties, and functional phylogenetics of light-sensitive protein modules. Moreover, investigations from the neuroscience side will fundamentally advance the scope and precision of resulting insights into complex intact biological systems (Fig. 4). These investigations will explore targeting, trafficking, selective spatiotemporal properties of illumination, precise circuit-element recruitment, and diverse readout engineering and analysis. In optogenetics, existing methods represent only the tip of the iceberg in terms of what may be ultimately achieved in maximally enabling this technique's principled design and application.

References

Airan RD, Thompson KR, Fenno LE, Bernstein H, Deisseroth K (2009) Temporally precise *in vivo* control of intracellular signalling. Nature 458:1025–1029.

© 2013 Deisseroth

NOTES

Boyden ES, Zhang F, Bamberg E, Nagel G, Deisseroth K (2005) Millisecond-timescale, genetically targeted optical control of neural activity. Nat Neurosci 8:1263–1268.

Fenno LE, Deisseroth K (2013) Optogenetic technologies for psychiatric disease research. In: Neurobiology of mental illness, 4th ed. (Charney D, Nestler E, Sklar P, Nestler EJ, eds). New York: Oxford UP.

Gradinaru V, Thompson KR, Deisseroth K (2008) eNpHR: a Natronomonas halorhodopsin enhanced for optogenetic applications. Brain Cell Biol 36:129–139.

Ishizuka T, Kakuda M, Araki R, Yawo H (2006) Kinetic evaluation of photosensitivity in genetically engineered neurons expressing green algae light-gated channels. Neurosci Res 54:85–94.

Kato H, Zhang F, Yizhar O, Ramakrishnan C, Nishizawa T, Hirata K, Ito J, Aita Y, Tsukazaki T, Hayashi S, Hegemann P, Maturana A, Ishitani R, Deisseroth K, Nureki O (2012) Crystal structure of the channelrhodopsin light-gated cation channel. Nature 482:369–374.

Lin JY, Lin MZ, Steinbach P, Tsien RY (2009) Characterization of engineered channelrhodopsin variants with improved properties and kinetics. Biophys J 96:1803–1814.

Mattis J, Tye K, Ferenczi E (2012) Principles for applying optogenetic tools derived from direct comparative analysis of microbial opsins. Nat Methods 9:159–172.

Möglich A, Moffat K (2007) Structural basis for light-dependent signaling in the dimeric LOV domain of the photosensor YtvA. J Mol Biol 373:112–126.

Packer AM, Peterka DS, Hirtz JJ, Prakash R, Deisseroth K, Yuste R (2012) Two-photon optogenetics of dendritic spines and neuronal circuits. Nat Methods 9:1202–1205.

Prakash R, Yizhar O, Grewe B, Ramakrishnan C, Wang N, Goshen I, Packer AM, Peterka DS, Yuste R, Schnitzer MJ, Deisseroth K (2012) Two-photon optogenetic toolbox for fast inhibition, excitation and bistable modulation. Nat Methods 9:1171–1179.

Stehfest K, Hegemann P (2010) Evolution of the channelrhodopsin photocycle model. Chem Phys Chem 11:1120–1126.

Stierl M, Stumpf P, Udwari D, Gueta R, Hagedorn R, Losi A, Gartner W, Petereit L, Efetova M, Schwarzel M, Oertner TG, Nagel G, Hegemann P (2011) Light modulation of cellular cAMP by a small bacterial photoactivated adenylyl cyclase, bPAC, of the soil bacterium *Beggiatoa*. J Biol Chem 286:1181–1188.

Wu YI, Frey D, Lungu OI, Jaehrig A, Schlichting I, Kuhlman B, Hahn KM (2009) A genetically encoded photoactivatable Rac controls the motility of living cells. Nature 461:104–108.

Yizhar O, Fenno LE, Davidson TJ, Mogri M, Deisseroth K (2011) Optogenetics in neural systems. Neuron 71:9–34.

Zalocusky KA, Deisseroth K (2013) Optogenetics in the behaving rat: integration of diverse new technologies in a vital animal model. Optogenetics 1:1–17.

Zhang F, Vierock J, Yizhar O, Fenno LE, Tsunoda S, Kianianmomeni A, Prigge M, Berndt A, Cushman J, Polle J, Magnuson J, Hegemann P, Deisseroth K (2011) The microbial opsin family of optogenetic tools. Cell 147:1446–1457.

© 2013 Deisseroth

Remote Control of Cellular Signaling Using DREADD Technology

Bryan L. Roth MD, PhD

Department of Pharmacology
University of North Carolina Chapel Hill Medical School
Chapel Hill, North Carolina

© 2013 Roth

NOTES

Introduction

In his visionary review of 1979, Francis Crick suggested that a major goal of neuroscience is to identify "which features (of the brain) it would be most useful to study and in particular to measure" (Crick, 1979). To identify and perturb these features in a productive way, it would be necessary to invent a method "by which *all neurons of just one type could be inactivated*, leaving the others more or less unaltered" [emphasis mine] (Crick, 1979). Sometime later, he expanded this wish list to include the ability "to turn the firing of one or more types of neuron on and off in the alert animal in a rapid manner" (Crick, 1999). The idea Crick proposed, then, was that in order to begin to construct a wiring diagram of neuronal circuits involved in regulating particular behaviors, there was a pressing need for a way to reversibly regulate neuronal activity in a cell-type-specific manner.

During the past 10 years, a number of technologies have been developed to achieve the cell-type-specific and reversible modulation of neuronal activity he envisioned. These include the following:

- Light-activated channels for activating (Nagel et al., 2002, 2003, 2005; Boyden et al., 2005) and silencing (Li et al., 2005; Zhang et al., 2007) neurons;
- Photochemical activation of neurons (Zemelman et al., 2002, 2003; Kokel et al., 2013);
- Chemogenetic or pharmacogenetic activation of neurons via engineered receptor–ligand pairs (Alexander et al., 2009); and
- Chemogenetic or pharmacogenetic inactivation of neurons via insect receptor–ligand pairs (Lechner et al., 2002) or engineered receptor–ligand pairs (Armbruster et al., 2007).

In a similar way, in order to understand how signaling processes in neuronal and nonneuronal cells regulate behavior, we will need tools that allow for precise spatiotemporal control of neuronal and nonneuronal signaling in a reversible, temporally controllable fashion. Thus, the aim of this research is to insert engineered receptors into specific neuronal populations and then to activate or inactivate them to discover how signaling processes regulate behavior in freely moving animals (Fig. 1).

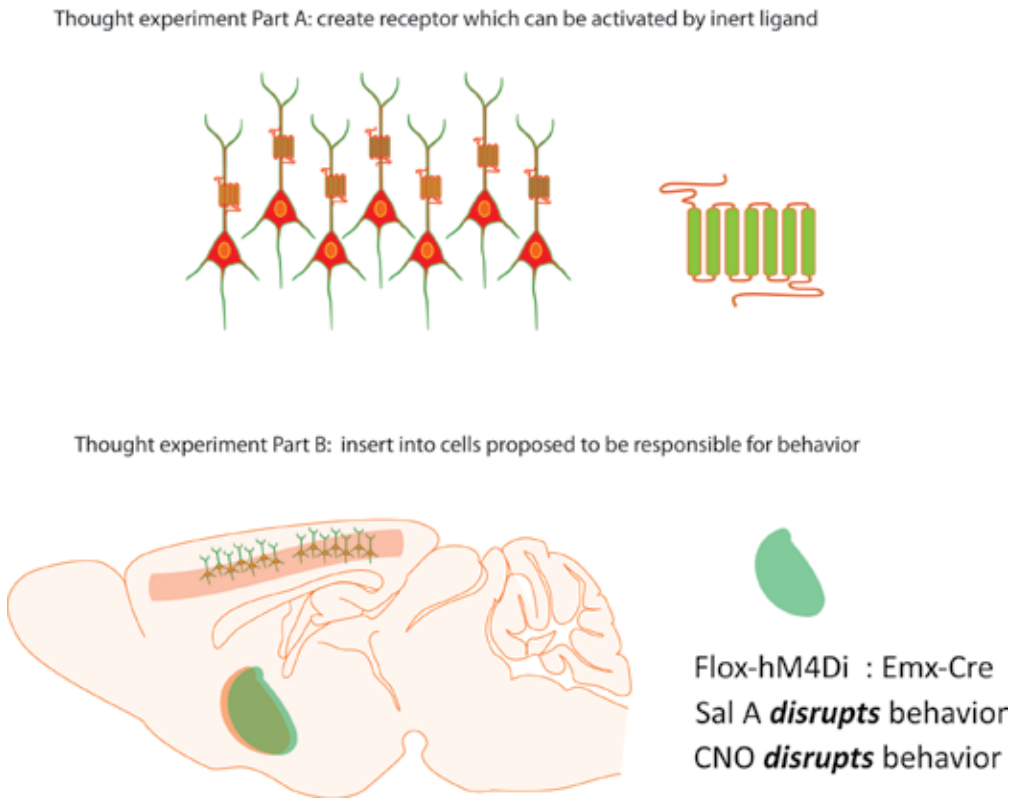

Figure 1. "Thought experiments" for using engineered GPCRs inserted into specific cells to interrogate signaling processes essential for behavior. Ideally, by inserting an engineered G_i-coupled receptor into cortical neurons via the Cre-Lox system, one can induce a behavior reminiscent of that induced by the κ-opioid–selective ligand salvinorin A. CNO, clozapine-*N*-oxide; Sal A, salvinorin A.

© 2013 Roth

NOTES

Table 1. Representative chemogenetic technologies for the remote control of cellular signaling

Technology		Ligand (s)	Outcome	Reference
Allele-specific control of GPCR signaling via engineered β-adrenergic receptor–ligand pair	β2-adrenergic receptor Asp^{113}->Ser^{113} mutant	1-(3',4'-dihydroxyphenyl)-3-methyl-L-butanone (L-185,870)	Reversible activation of G_s canonical signaling	Strader et al., 1991
RASSL–G_i (receptors activated solely by synthetic ligands)	κ-opioid chimeric receptor	Spiradoline (small-molecule κ-opioid agonist)	Reversible activation of canonical G_i signaling	Coward et al., 1998
Engineered receptor–ligand pairs to reversibly inactivate signaling	5-HT_{2A} serotonin receptor Phe^{340}->Leu^{340} mutant receptor	Inactive ketanserin analogues	Reversible inhibition of G_q signaling	Westkaemper et al., 1999
TREK (therapeutic receptor–effector complex) β-adrenergic receptor mutant	Extensive modifications of β2-adrenergic receptor	L-158,870	Reversible G_s activation	Small et al., 2001
Neoceptors	Engineered adenosine receptors	Inactive adenosine receptor ligands	Reversible activation of canonical adenosine signaling	Jacobson et al., 2001
RASSL-G_s	Melanocortin-4 receptor mutants	Small-molecule MC4 agonists	Reversible activation of G_s signaling	Srinivasan et al., 2003
G_i and G_q-DREADD	M_1, M_2, M_3, M_4, M_5-muscarinic receptor mutants	Inactive clozapine metabolite clozapine-*N*-oxide (CNO)	Reversible activation of G_i or G_q signaling	Armbruster et al., 2007
G_s-DREADD	Engineered M_3-muscarinic receptor	Inactive clozapine metabolite CNO	Reversible activation of G_s signaling	Guettier et al., 2009
Arrestin-DREADD	Engineered M_3-muscarinic receptor	Inactive clozapine metabolite CNO	Reversible activation of arrestin signaling	Nakajima and Wess, 2012

Activating G-Protein Coupled Receptors

During the past 20 or more years, a number of tools have been developed that allow for the reversible activation of G-protein coupled receptors (GPCRs) (Table 1) (Conklin et al., 2008; Rogan and Roth, 2011). These have been various dubbed "allele-specific genetically engineered receptors" (Strader et al., 1991); "receptors activated solely by synthetic ligands" (RASSLs) (Coward et al., 1998); "engineered receptors" (Westkaemper et al., 1999); "therapeutic receptor–effector complexes" (TREKs) (Small et al., 2001); "neoceptors" (Jacobson et al., 2001); and "designer receptors exclusively activated by designer drugs" (DREADD) (Armbruster et al., 2007). Among these variations on the theme of engineered GPCR–ligand pairs, DREADDs have emerged as the most frequently used tool for remotely controlling neuronal signaling. This chapter focuses on the specific application of DREADD technology.

Figure 2. Point mutations essential for creation of DREADD receptors. Shown are the locations of the two-point mutations (Y149C$^{(3.33)}$, A239G$^{(5.46)}$) that are conserved residues within all acetylcholine muscarinic receptors, including *Drosophila*.

Designer Receptors Exclusively Activated by Designer Drugs—DREADDs

DREADDs were originally invented by modifying muscarinic acetylcholine receptors to be activated by the inert ligand clozapine-*N*-oxide (CNO) via directed molecular evolution in genetically engineered yeast (Armbruster et al., 2007). In the process, two-point mutations of highly conserved amino acids (Y3.33C and A5.46G via the Ballesteros and Weinstein numbering convention; Ballesteros and Weinstein, 1995) rendered all 5 human muscarinic receptors both unable to be

© 2013 Roth

NOTES

Table 2. Representative experiments using DREADDs to modulate behavior by remote cell-type-specific control of neuronal signaling

DREADD	Experiment	Result	References
hM_3D_q +/– hM_4D_i	Remote control of feeding	Identification of neurons that encode hunger	Krashes et al., 2011; Atasoy et al., 2012
hM_3D_q	Generation of a synthetic memory trace	Memory encoded sparsely	Garner et al., 2012
hM_4D_i	Alteration in neuronal plasticity	Altered striatal connectivity	Kozorovitskiy et al., 2012
hM_4D_i	5-HT neuron silencing	Behavior and physiological consequences	Ray et al., 2011
hM_3D_q	Identification of neurons responsible for pleasurable sensation	DRG neurons identified as target of MGPR4 orphan receptor	Vrontou et al., 2013
G_sD	Modulation of cAMP	Modulates circadian clock	Brancaccio et al., 2013

activated by acetylcholine (their endogenous agonist) and exquisitely sensitive to CNO (Fig. 2).

To date, DREADDs suitable for remotely activating the designer receptors G_i (e.g., hM_4G_i) (Armbruster et al., 2007), G_q (e.g., hM_3G_q) (Armbruster et al., 2007), G_s (e.g., G_sD) (Guettier et al., 2009) and arrestin (e.g., Arr-DREADD) (Nakajima and Wess, 2012) signaling have been reported. These are activated using the pharmacologically inactive compound and clozapine metabolite CNO and have been extensively validated (Table 1). In all neuron types reported to date:

- Activation of the hM_3D_q by CNO induces neuronal depolarization and burst firing (Alexander et al., 2009; Krashes et al., 2011; Atasoy et al., 2012);
- Activation of hM_4D_i by CNO induces neuronal hyperpolarization and silencing (Armbruster et al., 2007; Krashes et al., 2011; Atasoy et al., 2012);
- Activation of G_sD by CNO enhances neuronal Gs signaling (Brancaccio et al., 2013; Farrell et al., 2013); and
- CNO has no effect on baseline firing (Alexander et al., 2009; Krashes et al., 2011; Atasoy et al., 2012) or signaling in neurons not expressing DREADDs (Brancaccio et al., 2013; Farrell et al., 2013).

(There have been no reports on the utility of the arrestin-specific DREADD for remotely controlling neuronal arrestin signaling.)

The mechanism(s) responsible for these alterations in neuronal activity are unknown. However, the hyperpolarization of neurons and inhibition of firing by hM_4D_i is likely caused in part by the activation of G-protein inwardly rectifying potassium channels (Armbruster et al., 2007). To date, a large number of investigators have reported success in using DREADD technology to selectively modulate neuronal signaling and firing (Table 2).

Pros and Cons of DREADD Technology

DREADDs are now widely used in neuroscience to remotely control neuronal signaling. DREADDs offer the following advantages over other, more invasive technologies such as optogenetics:

- They are able to noninvasively control neuronal and nonneuronal signaling, as CNO can be administered peripherally via injection (Alexander et al., 2009) or through drinking water (D.J. Urban and B.L. Roth, unpublished observations) (protocols available at http://dreadd.org/);
- They can modulate signaling and activity of widely dispersed neurons (Garner et al., 2012);
- They can modulate signaling and activity of optically inaccessible neurons (Vrontou et al., 2013);
- They can be used to modulate activity of neurons early in development in a noninvasive manner (Kozorovitskiy et al., 2012);
- They are appropriate for long-term studies (e.g., days to weeks) (Farrell et al., 2013); and
- CNO-modulated activity can last hours after a single injection (Alexander et al., 2009).

The main disadvantage DREADD technology as compared with optical technologies is the lack of precise, millisecond control of activity. Although it is likely that "caging" CNO is possible (B.L. Roth, unpublished observations) so that millisecond control can be achieved by photochemically uncaging CNO, optical technologies will likely remain the most useful under conditions in which precise millisecond control of neuronal activity is needed.

© 2013 Roth

NOTES

Summary

DREADD technology has emerged as a facile approach for remotely and noninvasively controlling neuronal and nonneuronal signaling. CNO-induced activation of hM_3D_q triggers neuronal burst firing and, accordingly, hM_3D_q is frequently used to remotely activate neurons. The activation of hM_4D_i by CNO can silence neurons and, accordingly, hM_4D_i is frequently used to remotely inactive neuronal activity. The development of additional DREADDs, as well as DREADDs that selectively activate distinct downstream effectors, will greatly expand our ability to remotely control and interrogate neuronal signaling in both health and disease.

References

Alexander GM, Rogan SC, Abbas AI, Armbruster BN, Pei Y, Allen JA, Nonneman RJ, Hartmann J, Moy SS, Nicolelis MA, McNamara JO, Roth BL (2009) Remote control of neuronal activity in transgenic mice expressing evolved G protein-coupled receptors. Neuron 63:27–39.

Armbruster BN, Li X, Pausch MH, Herlitze S, Roth BL (2007) Evolving the lock to fit the key to create a family of G protein-coupled receptors potently activated by an inert ligand. Proc Natl Acad Sci USA 104:5163–5168.

Atasoy D, Betley JN, Su HH, Sternson SM (2012) Deconstruction of a neural circuit for hunger. Nature 488:172–177.

Ballesteros JA, Weinstein H (1995) Integrated methods for the construction of three-dimensional models and computational probing of structure-function relations in G protein-coupled receptors. In: Methods in neurosciences (Sealfon SC, Conn PM, eds), pp 366–428. San Diego, CA: Academic Press.

Boyden ES, Zhang F, Bamberg E, Nagel G, Deisseroth K (2005) Millisecond-timescale, genetically targeted optical control of neural activity. Nat Neurosci 8:1263–1268.

Brancaccio M, Maywood ES, Chesham JE, Loudon AS, Hastings MH (2013) A gq-ca(2+) axis controls circuit-level encoding of circadian time in the suprachiasmatic nucleus. Neuron 78:714–728.

Conklin BR, Hsiao EC, Claeysen S, Dumuis A, Srinivasan S, Forsayeth JR, Guettier JM, Chang WC, Pei Y, McCarthy KD, Nissenson RA, Wess J, Bockaert J, Roth BL (2008) Engineering GPCR signaling pathways with RASSLs. Nat Methods 5:673–678.

Coward P, Wada HG, Falk MS, Chan SD, Meng F, Akil H, Conklin BR (1998) Controlling signaling with a specifically designed Gi-coupled receptor. Proc Natl Acad Sci USA 95:352–357.

Crick FH (1979) Thinking about the brain. Sci Am 241:219–232.

Crick F (1999) The impact of molecular biology on neuroscience. Philos Trans R Soc Lond B Biol Sci 354:2021–2025.

Farrell MS, Pei Y, Wan Y, Yadav PN, Daigle TL, Urban DJ, Lee HM, Sciaky N, Simmons A, Nonneman RJ, Huang XP, Hufeisen SJ, Guettier JM, Moy SS, Wess J, Caron MG, Calakos N, Roth BL (2013) A Galphas DREADD mouse for selective modulation of cAMP production in striatopallidal neurons. Neuropsychopharmacology 38:854–862.

Garner AR, Rowland DC, Hwang SY, Baumgaertel K, Roth BL, Kentros C, Mayford M (2012) Generation of a synthetic memory trace. Science 335:1513–1516.

Guettier JM, Gautam D, Scarselli M, Ruiz de Azua I, Li JH, Rosemond E, Ma X, Gonzalez FJ, Armbruster BN, Lu H, Roth BL, Wess J (2009) A chemical-genetic approach to study G protein regulation of beta cell function *in vivo*. Proc Natl Acad Sci USA 106:19197–19202.

Jacobson KA, Gao ZG, Chen A, Barak D, Kim SA, Lee K, Link A, Rompaey PV, van Calenbergh S, Liang BT (2001) Neoceptor concept based on molecular complementarity in GPCRs: a mutant adenosine A(3) receptor with selectively enhanced affinity for amine-modified nucleosides. J Med Chem 44:4125–4136.

Kokel D, Cheung CY, Mills R, Coutinho-Budd J, Huang L, Setola V, Sprague J, Jin S, Jin YN, Huang XP, Bruni G, Woolf CJ, Roth BL, Hamblin MR, Zylka MJ, Milan DJ, Peterson RT (2013) Photochemical activation of TRPA1 channels in neurons and animals. Nat Chem Biol 9:257–263.

Kozorovitskiy Y, Saunders A, Johnson CA, Lowell BB, Sabatini BL (2012) Recurrent network activity drives striatal synaptogenesis. Nature 485:646–650.

Krashes MJ, Koda S, Ye C, Rogan SC, Adams AC, Cusher DS, Maratos-Flier E, Roth BL, Lowell BB (2011) Rapid, reversible activation of AgRP neurons drives feeding behavior. J Clin Invest 121:1424–1428.

© 2013 Roth

NOTES

Lechner HA, Lein ES, Callaway EM (2002) A genetic method for selective and quickly reversible silencing of mammalian neurons. J Neurosci 22:5287–5290.

Li X, Gutierrez DV, Hanson MG, Han J, Mark MD, Chiel H, Hegemann P, Landmesser LT, Herlitze S (2005) Fast noninvasive activation and inhibition of neural and network activity by vertebrate rhodopsin and green algae channelrhodopsin. Proc Natl Acad Sci USA 102:17816–17821.

Nagel G, Ollig D, Fuhrmann M, Kateriya S, Musti AM, Bamberg E, Hegemann P (2002) Channelrhodopsin-1: a light-gated proton channel in green algae. Science 296:2395–2398.

Nagel G, Szellas T, Huhn W, Kateriya S, Adeishvili N, Berthold P, Ollig D, Hegemann P, Bamberg E (2003) Channelrhodopsin-2, a directly light-gated cation-selective membrane channel. Proc Natl Acad Sci USA 100:13940–13945.

Nagel G, Brauner M, Liewald JF, Adeishvili N, Bamberg E, Gottschalk A (2005) Light activation of channelrhodopsin-2 in excitable cells of *Caenorhabditis elegans* triggers rapid behavioral responses. Curr Biol 15:2279–2284.

Nakajima K, Wess J (2012) Design and functional characterization of a novel, arrestin-biased designer G protein-coupled receptor. Mol Pharmacol 82:575–582.

Ray RS, Corcoran AE, Brust RD, Kim JC, Richerson GB, Nattie E, Dymecki SM (2011) Impaired respiratory and body temperature control upon acute serotonergic neuron inhibition. Science 333:637–642.

Rogan SC, Roth BL (2011) Remote control of neuronal signaling. Pharmacol Rev 63:291–315.

Small KM, Brown KM, Forbes SL, Liggett SB (2001) Modification of the beta 2-adrenergic receptor to engineer a receptor-effector complex for gene therapy. J Biol Chem 276:31596–31601.

Srinivasan S, Vaisse C, Conklin BR (2003) Engineering the melanocortin-4 receptor to control G(s) signaling *in vivo*. Ann NY Acad Sci 994:225–232.

Strader CD, Gaffney T, Sugg EE, Candelore MR, Keys R, Patchett AA, Dixon RA (1991) Allele-specific activation of genetically engineered receptors. J Biol Chem 266:5–8.

Vrontou S, Wong AM, Rau KK, Koerber HR, Anderson DJ (2013) Genetic identification of C fibres that detect massage-like stroking of hairy skin *in vivo*. Nature 493:669–673.

Westkaemper R, Glennon R, Hyde E, Choudhary M, Khan N, Roth B (1999) Engineering a region of bulk tolerance into the 5-HT_{2A} receptor. Eur J Med Chem 34:441–447.

Zemelman BV, Lee GA, Ng M, Miesenbock G (2002) Selective photostimulation of genetically chARGed neurons. Neuron 33:15–22.

Zemelman BV, Nesnas N, Lee GA, Miesenbock G (2003) Photochemical gating of heterologous ion channels: remote control over genetically designated populations of neurons. Proc Natl Acad Sci USA 100:1352–1357.

Zhang F, Wang LP, Brauner M, Liewald JF, Kay K, Watzke N, Wood PG, Bamberg E, Nagel G, Gottschalk A, Deisseroth K (2007) Multimodal fast optical interrogation of neural circuitry. Nature 446:633–639.

© 2013 Roth

Optogenetic Modulation of Neural Circuits That Underlie Reward-Seeking

Garret D. Stuber, PhD

Departments of Psychiatry and Cell and Molecular Physiology
UNC Neuroscience Center
University of North Carolina at Chapel Hill
Chapel Hill, North Carolina

© 2013 Stuber

NOTES

Introduction

The manifestation of complex neuropsychiatric disorders, such as drug and alcohol addiction, is thought to result from progressive maladaptive alterations in neural circuit function. Repeated drug exposure has been shown to alter a distributed network of neural circuit elements. However, a more precise understanding of addiction has been hampered by an inability to control and, consequently, to identify specific circuit components that underlie addictive behaviors. The development of optogenetic strategies for selectively modulating the activity of genetically defined neuronal populations has provided a means for determining the relationship between circuit function and behavior with a level of precision that was previously unobtainable.

In this chapter, we briefly review the main optogenetic studies that have contributed to elucidating neural circuit connectivity within the ventral tegmental area (VTA) and the nucleus accumbens (NAc)—two brain nuclei that are essential for the manifestation of addiction-related behaviors. Additional targeted manipulation of genetically defined neural populations in these brain regions, as well as afferent and efferent structures, promises to delineate the cellular mechanisms and circuit components required for an organism to transition from natural goal-directed behavior to compulsive reward-seeking, despite its negative consequences.

Optogenetics for Studying Complex Neural Systems

The organizational complexity of the brain is both a source of its computational power and the main obstacle to our understanding neural systems and the development of therapeutics for neuropsychiatric diseases, such as addiction. Although the basic neuroanatomical substrates required for reward-related behavior have been identified, the specific function of genetically defined neurons and neural circuits remains unclear. To define the functional connectivity between neurons and their role in modulating complex behaviors, such as reward-seeking, requires the ability to perturb specific neural circuits on physiologically relevant timescales. Given the complexity and high degree of interconnectivity within neural tissue, manipulating the activity of a single, genetically defined neuronal cell type in heterogeneous tissue has been a major obstacle. The development of optogenetic strategies, however, has allowed for selective activation and inhibition of genetically defined circuit elements with millisecond resolution. This ability has circumvented many of the technical limitations of traditional techniques used in systems and behavioral neuroscience research. A new level of mechanistic insight into the neural underpinnings of motivated behaviors is now possible.

Two highly interconnected brain regions play critical roles in mediating reward-seeking behaviors, including those related to addiction: the VTA and the NAc. These brain regions comprise multiple, genetically distinct cell groups that integrate and convey reward-related information. The following sections briefly introduce the use of optogenetics to study neural circuit function. Next, they provide an overview of the synaptic connectivity within the VTA and NAc and highlight how optogenetic studies have further delineated neural circuit function within these regions.

Tools and Strategies for Optogenetic Manipulation of Neural Circuits That Underlie Reward Processing

Several optogenetic actuators are now available for both excitation and inhibition of neural circuits for use both *in vitro* and *in vivo* (Yizhar et al., 2001). To date, the most commonly used light-gated proteins for activating neural tissue are engineered mutants of channelrhodopsin-2 (ChR2) (Boyden et al., 2005). ChR2 mutants are typically maximally activated by 450–500 nm light, which allows for large inward flux of Na^+ and Ca^{2+} at resting membrane potentials. Brief pulses of light (typically 1–5 ms) result in reliable and repeatable action potential generation in a variety of neuronal subtypes over a large range of firing frequencies (Tsai et al., 2009; Stuber et al., 2011). Expression of ChR2 in neuronal fibers can also be used to selectively activate pathway-specific neurotransmitter release in brain slices (Petreanu et al., 2007; Stuber et al., 2010, 2011) or in behaving animals (Stuber et al., 2011; Tye et al., 2011) to study the effects of afferent-specific synaptic transmission. For optogenetic inhibition studies, modified variants of both halorhodopsin (Han et al., 2007; Zhang et al., 2007; Gradinaru et al., 2010) and archaerhodopsin (Chow et al., 2010; Han et al., 2011) have been shown to reliably silence neural activity both *in vitro* and *in vivo*. Transgenes coding for gated proteins to modulate neural activity are typically introduced into neural tissue via transgenic animals that express these proteins under cell-type-specific neuronal promoters (Wang et al., 2007; Zhao et al., 2011), or, more commonly, by recombinant viral vectors that can be stereotactically delivered to discrete brain nuclei. For delivering light to neural tissue *in vivo*, optical fibers, coupled with high-powered light sources such as lasers or LEDs, are used (Cardin et

© 2013 Stuber

NOTES

al., 2010; Zhang et al., 2010; Sparta et al., 2011). This provides a way to restrict light delivery and thus optical modulation to specific brain structures. Combined with genetic targeting approaches to selectively express these light-activated proteins in genetically defined neurons (Tsai et al., 2009), use of these tools allows for selective modulation of neural circuits that underlie reward-related behaviors.

Neuronal Populations in the VTA and Their Role in Mediating Reward-Seeking Behavior

The VTA is a heterogeneous brain structure containing neuronal populations that are essential to the expression of motivated behaviors related to addiction (Wise, 2004; Fields et al., 2007). While the VTA is often treated as a distinct neural structure, few anatomical markers distinguish it from neighboring structures such as the substantia nigra pars compacta (SNc). Immunohistochemical and tracing studies have suggested that the SNc comprises a relatively homogenous population of neurons, the majority of which are dopaminergic (DAergic) (90%) and project to the dorsal striatum (Swanson, 1982; Margolis et al., 2006). The VTA, on the other hand, contains a mixture of DAergic (~65%), GABAergic (~30%), and glutamatergic neurons (~5%) (Dobi et al., 2010) that project throughout the forebrain to structures including the amygdala, prefrontal cortex, and NAc (Swanson, 1982). Importantly, VTA neurons that project to the NAc are a heterogeneous population of both DAergic and GABAergic neurons (Van Bockstaele and Pickel, 1995; Carr and Sesack, 2000a; Margolis et al., 2006). Within the VTA, GABAergic neurons also are thought to form inhibitory contacts onto at least some DAergic projection neurons (Johnson and North, 1992). Thus, VTA GABAergic neurons, as well as GABAergic input from the posterior segment of the VTA, also known as the rostromedial tegmental nucleus (RMTg) (Jhou et al., 2009a,b), may play an important role in regulating DAergic neuron function. These diverse neuronal populations in the VTA are likely components of distinct neural circuits incorporating neurons from their afferent and efferent structures (discussed in detail below), which may act to mediate specific aspects of motivated behavioral processing (Lammel et al., 2011).

The pioneering optogenetic studies in this field introduced the blue light–sensitive cation channel ChR2 exclusively into VTA DAergic neurons using viral delivery methods to examine the role of these specific VTA neurons in reward-seeking behavior (Tsai et al., 2009; Brown et al., 2010; Stuber et al., 2010; Aamantidis et al., 2011). While the actions of DA were known to play an important role in reward-related behaviors, it was not possible to study how the selective activation of DAergic neurons alone could modulate reward-related behavior. Noncontigent, high-frequency, optical activation of VTA DAergic neurons led to the formation of a conditioned place preference (CPP) to the associated environment (Tsai et al., 2009). Significantly, DAergic stimulation frequencies that led to the development of a CPP also resulted in transient surges of DA release in the NAc, suggesting that only stimulation frequencies that lead to detectable changes in DA release can induce associative learning. In addition, it has been demonstrated that direct optical activitation of these neurons can reinforce operant behavioral responding (Witten et al., 2011) and facilitate the development of positive reinforcment (Adamantidis et al., 2011). Taken together, these studies demonstrate that direct activation of VTA DAergic neurons alone can promote behavioral conditioning and reinforce behavioral response in the absence of any additional reward.

Optogenetic strategies have also been employed in brain-slice experiments to examine the possibility of neurotransmitter corelease. Neurons in the medial VTA coexpress tyrosine hyrodylase and the vesicular glutamate transporter-2 (VGluT2), indicating that they are capable of both synthesizing DA and packaging glutamate into synaptic vesicles (Hnasko et al., 2010). Prior to optogenetic manipulations, however, it was not possible to selectively stimulate DAergic fibers originating from VTA neurons to determine whether they corelease dopamine and other small-molecule neurotransmitters. Optogenetic stimulation of DAergic terminals in the NAc led to detectable glutamate-mediated excitatory postsynaptic currents (Stuber et al., 2010; Tecuapetla et al., 2010) that were not present in mice that lack VGluT2 in DAergic neurons (Stuber et al., 2010). Further, glutamate release was not detected in dorsal striatal regions despite optogenetic stimulation of DAergic fibers producing detectable DA release (Stuber et al., 2010). These studies suggest that midbrain DAergic neurons that project to the ventral but not dorsal striatum can corelease glutamate as a neurotransmitter. Interestingly, a recent electron microscopy study demonstrated that axonal fibers within different striatal subregions do not coexpress TH and VGlutT1, VGlutT2, or VglutT3 (Moss et al., 2011). These results suggest there may be major species-specific differences in the neurotransmitter content of DAergic neurons (the

© 2013 Stuber

NOTES

optogenetic studies were performed in mice, whereas the electron microscopy study was performed in rats). However, it is worth noting that cultured DAergic neurons from rats also corelease glutamate (Sulzer et al., 1998; Joyce and Rayport, 2000) and that electrical stimulation of the VTA results in glutamate-mediated EPSPs in the prefrontal cortex of rats (Lavin et al., 2005). These findings suggest that DAergic neurons in species other than mice also corelease glutamate. It is possible that different axonal fibers that orginate from a single DAergic neuron in the VTA may release DA or glutmate, but not both. In addition, transcriptional suppression of TH may occur in VTA neurons that coexpress VGluT2. Although further studies are required, these ideas could account for the discrepancies between the optogenetic studies demonstrating DA/glutamate corelease and the electron microscopy data showing that axonal fibers in the striatum do not coexpress TH and VGlut isoforms.

Excitatory afferent projections to the VTA

Direct optogenetic stimulation of VTA DAergic neurons has demonstrated unequivocally that activation of these neurons is sufficient to modulate reward-related behaviors. Thus, an important line of research that remains largely unexplored is determining how specific VTA afferents modulate the activity of both DAergic and non-DAergic neurons in the VTA. Both excitatory and inhibitory afferents from a number of nuclei (Fig. 1) innervate postsynaptic neurons within the VTA. The heterogeneity of these inputs is such that electrical stimulation cannot be used to activate specific presynaptic fibers. Therefore, future studies will have to rely on afferent-specific optogenetic stimulation to study pathway-specific synaptic function in the VTA. Optogenetic stimulation of presynaptic fibers in other brain regions has already uncovered novel functions of afferent-specific inputs (Petreanu et al., 2007; Stuber et al., 2011; Tye et al., 2011). Exposure to many drugs and natural rewards can alter excitatory synaptic function onto midbrain DAergic neurons (Ungless et al., 2001; Saal et al., 2003; Borgland et al., 2004; Bellone and Luscher, 2006; Mameli et al., 2007; Chen et al., 2008; Stuber et al., 2008; Lammel et al., 2011). Therefore, further identifying the exact synaptic connectivity to different populations of VTA neurons should provide a framework for better understanding the synaptic mechanism by which natural rewards and drug abuse alter synaptic function within the VTA.

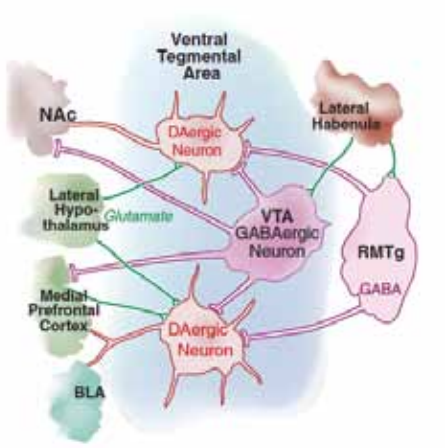

Figure 1. Circuitry of the ventral tegmental area. VTA DAergic neurons project to forebrain targets such as the basolateral amygdalae (BLA), mPFC, and NAc. These neurons received excitatory synaptic inputs from the LH, mPFC, and PPTg/LDT. Inhibitory inputs to the VTA neurons also arise from extended amygdala output structures. VTA GABAergic neurons target neighboring DAergic neurons as well as projecting to the mPFC and NAc. These neurons are thought to receive excitatory inputs from the LHb and inhibitory inputs from the NAc. RMTg, rostromedial tegmental nucleus. Reprinted from Stuber GD et al. (2012) *Biological Psychiatry*. 71(12):1061–1067, their Figure 1.

Lateral hypothalamus

The lateral hypothalamus (LH) is thought to send the largest subcortical glutamatergic projection to the VTA/SNc (Geisler et al., 2007). Electrical stimulation of the LH increases the firing rates predominately of VTA/SNc neurons that display long-duration action potential waveforms (Maeda and Mogenson, 1981). In contrast, neurons that show short-duration waveforms are generally suppressed by LH stimulation (Maeda and Mogenson, 1981). While most of the fibers originating from the LH and projecting to the VTA are glutamatergic (Geisler et al., 2007) and may corelease the neuropeptide orexin (Aston-Jones et al., 2010), whether there is a GABAergic input from the LH to the VTA is unknown. VTA-projecting LH neurons show increased activity as indexed by *c-fos* following cocaine or morphine CPP (Harris et al., 2005, 2007), and VTA neurons show increases in *c-fos* expression following LH stimulation (Arvanitogiannis et al., 1997). In addition, LH self-stimulation leads to large increases in NAc DA release (Hernandez and Hoebel, 1988), further demonstrating an important role of this pathway in the activation of brain reward circuits as well as reinforcing behavioral responding. Taken together, these studies show that the LH is an

© 2013 Stuber

NOTES

important source of excitatory drive to the VTA. It is hoped that future studies that involve afferent-specific optogenetic stimulation of LH afferents to the VTA will illuminate the synaptic connectivity between these regions as well as their role in reward-related behaviors.

Medial prefrontal cortex

Another major source of glutamatergic input to the VTA comes from a long-range projection from the medial prefrontal cortex (mPFC), which is thought to target both DAergic and non-DAergic neurons (Sesack and Pickel, 1992; Carr and Sesack, 2000b; Geisler et al., 2007). Stimulation of the mPFC performs a variety of functions: It leads to an increase in extracellular glutamate in the VTA (You et al., 2007), activates DAergic and non-DAergic neurons (Gariano and Groves, 1988; Tong et al., 1996; Moorman and Aston-Jones, 2010), and elevates DA release in the forebrain (Karreman and Moghaddam, 1996; You et al., 1998). Interestingly, an electron microscopy study by Carr and Sesack (2000b) showed that mPFC afferents to the VTA form synapses onto mPFC-projecting, but not NAc-projecting, DAergic neurons. mPFC afferents also formed synapses onto VTA GABAergic neurons that project to the NAc but not those that project to the mPFC. Afferent-specific optogenetic stimulation with postsynaptic recordings from DAergic and non-DAergic neurons in the VTA is needed to corroborate these findings.

Lateral habenula

The lateral habenula (LHb) is another major excitatory input to the VTA and an important modulator of DAergic neuronal activity (Christoph et al., 1986; Matsumoto and Hikosaka, 2007; Bromberg-Martin et al., 2010). Glutamatergic fibers originating in the LHb project directly to the VTA (Herkenham and Nauta, 1979; Geisler et al., 2007) and are thought to form synapses on both DAergic and GABAergic neurons there (Omelchenko et al., 2009). Interestingly, electrophysiological recordings from LHb neurons in behaving monkeys have demonstrated that these neurons are predominantly inhibited during reward expectation, while DAergic neurons in the midbrain show excitatory responses (Matsumoto and Hikosaka, 2007, 2009; Bromberg-Martin et al., 2010). In addition, LHb neurons are excited by aversive stimuli (Matsumoto and Hikosaka, 2007), and stimulation of the LHb leads to reduced DA release in the NAc (Lisoprawski et al., 1980). These studies suggest that LHb neurons send a direct glutamatergic projection to predominantly GABAergic neurons in the VTA/SNc that can inhibit DAergic neuronal activity.

Pedunculopontine tegmental nucleus

The VTA also receives a mixed glutamatergic/cholinergic projection from the pedunculopontine tegmental nucleus (PPTg) and the laterodorsal tegmental nucleus (LDT) (Hallanger and Wainer, 1988; Futami et al., 1995; Omelchenko and Sesack, 2005). Consistent with this, electrical stimulation of PPTg/LDT increases the activity of VTA neurons and increases DA release in the NAc (Floresco et al., 2003). While the PPTg/LDT plays an important role in driving drug-seeking behavior (Schmidt et al., 2009), how the synaptic connectivity between the PPTg/LDT and the VTA controls reward-related behaviors remains unknown.

Inhibitory Afferents to the VTA/SNc

Within the VTA, afferent-specific optogenetic stimulation experiments examining the synaptic connectivity between neurons have demonstrated that distal GABAergic neurons orginating in the NAc form functional inhibitory synaptic contacts onto non-DAergic neurons in the VTA (Xia et al., 2011). Furthermore, some non-DAergic neurons that receive inhibitory inputs from the NAc were shown to project back to the NAc (Xia et al., 2011). This study elegantly demonstrated the precise functional inhibitory connectivity between the NAc to VTA GABAergic neurons. Other neurons throughout the extended amydala, such as those from the central nucleus of the amygdala (CeA) and the bed nucleus of the stria terminalus (BNST), were also found to project to the VTA (Georges and Aston-Jones, 2001; Jalabert et al., 2009; Lee et al., 2011). While electrical stimulation of the BNST produces both excitatory and inhibitory responses in the VTA (Georges and Aston-Jones, 2001), we have recently demonstrated that the BNST sends a mixed glutamatergic and GABAergic projection that preferentially inneverates non-DAergic neurons in the VTA (Jennings et al., 2013). Local VTA GABAergic activity is also a potent modulator of DAergic output. The specific role for these distinct pathways in regulating VTA neural activity *in vivo* and during behavioral tasks should be explored further.

Conclusions

While optogenetic manipulations of brain reward circuitry have already helped establish and refute many hypotheses that were previously untestable with traditional techniques, studies that will expand our understanding of the mechanisms of neural circuits that underlie reward-seeking behavior are yet to come. Most of the studies reviewed utilized ChR2

© 2013 Stuber

for optogenetic stimulation of defined neuronal populations. While these early studies have certainly provided groundbreaking findings, many of them failed to take advantage of one of the greatest benefits of optogenetic methodologies: That is, they did not make use of transient activation or inactivation of neural tissue time-locked to discrete and infrequent behaviorally relevant events. In addition, while optogenetic stimulation experiments can demonstrate that synchronous activation of neurons can modulate behaviors related to reward-seeking, they do not demonstrate the necessity of specific neural circuit elements in behavior. Loss-of-function experiments utilizing optogenetic inhibition of neural circuits have lagged behind the adoption of ChR2-mediated stimulation, partially owing to technical limitations that have been recently overcome (Xia et al., 2011). These future studies will likely play a more prominent part in determining the role of specific connections between neurons in mediating motivated behavioral responses. Finally, a plethora of *in vivo* electrophysiological and neurochemical studies has elegantly shown correlations between neural activity and reward-seeking behavior. As optogenetic strategies for neural circuit manipulation are refined, these techniques to monitor neural activity will certainly become fully integrated with optogenetic circuit manipulation for assessing how neuronal actuation can alter neurophysiological and neurochemical responses observed during reward-seeking behavior. Taken together, it is likely that optogenetic strategies for perturbation of neural function, used in conjunction with sophisticated behavioral paradigms to study reward-seeking, will greatly enhance our understanding of the circuitry that mediates behavior.

Acknowledgments

G.D.S. was supported by grants from the National Alliance for Research on Schizophrenia and Depression (now the Brain and Behavior Research Foundation), the Alcoholic Beverage Medical Research Foundation, The Foundation of Hope, the Whitehall Foundation, the National Institute on Drug Abuse (DA029325), and startup funds provided by the Department of Psychiatry at UNC Chapel Hill. This chapter was adapted from Stuber GD, Britt JP, Bonci A (2012) Optogenetic modulation of neural circuits that underlie reward seeking. *Biological Psychiatry*. 71(12):1061–1067.

References

Adamantidis AR, Tsai HC, Boutrel B, Zhang F, Stuber GD, Budygin EA, Touriño C, Bonci A, Deisseroth K, de Lecea L (2011a) Optogenetic interrogation of dopaminergic modulation of the multiple phases of reward-seeking behavior. J Neurosci 31:10829–10835.

Arvanitogiannis A, Flores C, Shizgal P (1997) Fos-like immunoreactivity in the caudal diencephalon and brainstem following lateral hypothalamic self-stimulation. Behav Brain Res 88:275–279.

Aston-Jones G, Smith RJ, Sartor GC, Moorman DE, Massi L, Tahsili-Fahadan P, Richardson KA (2010) Lateral hypothalamic orexin/hypocretin neurons: A role in reward-seeking and addiction. Brain Res 1314:74–90.

Bellone C, Luscher C (2006) Cocaine triggered AMPA receptor redistribution is reversed *in vivo* by mGluR-dependent long-term depression. Nat Neurosci 9:636–641.

Borgland SL, Malenka RC, Bonci A (2004) Acute and chronic cocaine-induced potentiation of synaptic strength in the ventral tegmental area: electrophysiological and behavioral correlates in individual rats. J Neurosci 24:7482–7490.

Boyden ES, Zhang F, Bamberg E, Nagel G, Deisseroth K (2005) Millisecond-timescale, genetically targeted optical control of neural activity. Nat Neurosci 8:1263–1268.

Bromberg-Martin ES, Matsumoto M, Hikosaka O (2010) Distinct tonic and phasic anticipatory activity in lateral habenula and dopamine neurons. Neuron 67:144–155.

Brown MT, Bellone C, Mameli M, Labouèbe G, Bocklisch C, Balland B, Dahan L, Luján R, Deisseroth K, Lüscher C (2010) Drug-driven AMPA receptor redistribution mimicked by selective dopamine neuron stimulation. PLoS One 5:e15870.

Cardin JA, Carlen M, Meletis K, Knoblich U, Zhang F, Deisseroth K, Tsai LH, Moore CI (2010) Targeted optogenetic stimulation and recording of neurons *in vivo* using cell-type-specific expression of Channelrhodopsin-2. Nat Protoc 5:247–254.

Carr DB, Sesack SR (2000a) GABA-containing neurons in the rat ventral tegmental area project to the prefrontal cortex. Synapse 38:114–123.

Carr DB, Sesack SR (2000b) Projections from the rat prefrontal cortex to the ventral tegmental area: target specificity in the synaptic associations with mesoaccumbens and mesocortical neurons. J Neurosci 20:3864–3873.

NOTES

© 2013 Stuber

NOTES

Chen BT, Bowers MS, Martin M, Hopf FW, Guillory AM, Carelli RM, Chou JK, Bonci A (2008) Cocaine but not natural reward self-administration nor passive cocaine infusion produces persistent LTP in the VTA. Neuron 59:288–297.

Chow BY, Han X, Dobry AS, Qian X, Chuong AS, Li M, Henninger MA, Belfort GM, Lin Y, Monahan PE, Boyden ES (2010) High-performance genetically targetable optical neural silencing by light-driven proton pumps. Nature 463:98–102.

Christoph GR, Leonzio RJ, Wilcox KS (1986) Stimulation of the lateral habenula inhibits dopamine-containing neurons in the substantia nigra and ventral tegmental area of the rat. J Neurosci 6:613–619.

Dobi A, Margolis EB, Wang HL, Harvey BK, Morales M (2010) Glutamatergic and nonglutamatergic neurons of the ventral tegmental area establish local synaptic contacts with dopaminergic and nondopaminergic neurons. J Neurosci 30:218–229.

Fields HL, Hjelmstad GO, Margolis EB, Nicola SM (2007) Ventral tegmental area neurons in learned appetitive behavior and positive reinforcement. Annu Rev Neurosci 30:289–316.

Floresco SB, West AR, Ash B, Moore H, Grace AA (2003) Afferent modulation of dopamine neuron firing differentially regulates tonic and phasic dopamine transmission. Nat Neurosci 6:968–973.

Futami T, Takakusaki K, Kitai ST (1995) Glutamatergic and cholinergic inputs from the pedunculopontine tegmental nucleus to dopamine neurons in the substantia nigra pars compacta. Neurosci Res 21:331–342.

Gariano RF, Groves PM (1988) Burst firing induced in midbrain dopamine neurons by stimulation of the medial prefrontal and anterior cingulate cortices. Brain Res 462:194–198.

Geisler S, Derst C, Veh RW, Zahm DS (2007) Glutamatergic afferents of the ventral tegmental area in the rat. J Neurosci 27:5730–5743.

Georges F, Aston-Jones G (2001) Potent regulation of midbrain dopamine neurons by the bed nucleus of the stria terminalis. J Neurosci 21:RC160.

Gradinaru V, Zhang F, Ramakrishnan C, Mattis J, Prakash R, Diester I, Goshen I, Thompson KR, Deisseroth K (2010) Molecular and cellular approaches for diversifying and extending optogenetics. Cell 141:154–165.

Hallanger AE, Wainer BH (1988) Ascending projections from the pedunculopontine tegmental nucleus and the adjacent mesopontine tegmentum in the rat. J Comp Neurol. 274:483–515.

Han X, Boyden ES (2007) Multiple-color optical activation, silencing, and desynchronization of neural activity, with single-spike temporal resolution. PLoS One 2:e299.

Han X, Chow BY, Zhou H, Klapoetke NC, Chuong A, Rajimehr R, Yang A, Baratta MV, Winkle J, Desimone R, Boyden ES (2011) A high-light sensitivity optical neural silencer: development and application to optogenetic control of non-human primate cortex. Front Syst Neurosci 5:18.

Harris GC, Wimmer M, Aston-Jones G (2005) A role for lateral hypothalamic orexin neurons in reward seeking. Nature 437:556–559.

Harris GC, Wimmer M, Randall-Thompson JF, Aston-Jones G (2007) Lateral hypothalamic orexin neurons are critically involved in learning to associate an environment with morphine reward. Behav Brain Res 183:43–51.

Herkenham M, Nauta WJ (1979) Efferent connections of the habenular nuclei in the rat. J Comp Neurol 187:19–47.

Hernandez L, Hoebel BG (1988) Feeding and hypothalamic stimulation increase dopamine turnover in the accumbens. Physiol Behav 44:599–606.

Hnasko TS, Chuhma N, Zhang H, Goh GY, Sulzer D, Palmiter RD, Rayport S, Edwards RH (2010) Vesicular glutamate transport promotes dopamine storage and glutamate corelease *in vivo*. Neuron 65:643–656.

Jalabert M, Aston-Jones G, Herzog E, Manzoni O, Georges F (2009) Role of the bed nucleus of the stria terminalis in the control of ventral tegmental area dopamine neurons. Prog Neuropsychopharmacol Biol Psychiatry 33:1336–1346.

Jennings JH, Sparta DR, Stamatakis AM, Ung RL, Pleil KE, Kash TL, Stuber GD (2013) Distinct extended amygdala circuits for divergent motivational states. Nature 496:224–228.

Jhou TC, Fields HL, Baxter MG, Saper CB, Holland PC (2009a) The rostromedial tegmental nucleus (RMTg), a GABAergic afferent to midbrain dopamine neurons, encodes aversive stimuli and inhibits motor responses. Neuron 61:786–800.

Jhou TC, Geisler S, Marinelli M, Degarmo BA, Zahm DS (2009b) The mesopontine rostromedial tegmental nucleus: a structure targeted by the lateral habenula that projects to the ventral tegmental area of Tsai and substantia nigra compacta. J Comp Neurol 513:566–596.

© 2013 Stuber

NOTES

Johnson SW, North RA (1992) Opioids excite dopamine neurons by hyperpolarization of local interneurons. J Neurosci 12:483–488.

Joyce MP, Rayport S (2000) Mesoaccumbens dopamine neuron synapses reconstructed *in vitro* are glutamatergic. Neuroscience 99:445–456.

Karreman M, Moghaddam B (1996) The prefrontal cortex regulates the basal release of dopamine in the limbic striatum: an effect mediated by ventral tegmental area. J Neurochem 66:589–598.

Lammel S, Ion DI, Roeper J, Malenka RC (2011) Projection-specific modulation of dopamine neuron synapses by aversive and rewarding stimuli. Neuron 70:855–862.

Lavin A, Nogueira L, Lapish CC, Wightman RM, Phillips PE, Seamans JK (2005) Mesocortical dopamine neurons operate in distinct temporal domains using multimodal signaling. J Neurosci 25:5013–5023.

Lee HJ, Wheeler DS, Holland PC (2011) Interactions between amygdala central nucleus and the ventral tegmental area in the acquisition of conditioned cue-directed behavior in rats. Eur J Neurosci 33:1876–1884.

Lisoprawski A, Herve D, Blanc G, Glowinski J, Tassin JP (1980) Selective activation of the mesocortico-frontal dopaminergic neurons induced by lesion of the habenula in the rat. Brain Res 183:229–234.

Maeda H, Mogenson GJ (1981) A comparison of the effects of electrical stimulation of the lateral and ventromedial hypothalamus on the activity of neurons in the ventral tegmental area and substantia nigra. Brain Res Bull 7:283–291.

Mameli M, Balland B, Lujan R, Luscher C (2007) Rapid synthesis and synaptic insertion of GluR2 for mGluR-LTD in the ventral tegmental area. Science 317:530–533.

Margolis EB, Lock H, Hjelmstad GO, Fields HL (2006) The ventral tegmental area revisited: Is there an electrophysiological marker for dopaminergic neurons? J Physiol 577:907–924.

Matsumoto M, Hikosaka O (2007) Lateral habenula as a source of negative reward signals in dopamine neurons. Nature 447:1111–1115.

Matsumoto M, Hikosaka O (2009) Representation of negative motivational value in the primate lateral habenula. Nat Neurosci 12:77–84.

Moorman DE, Aston-Jones G (2010) Orexin/hypocretin modulates response of ventral tegmental dopamine neurons to prefrontal activation: diurnal influences. J Neurosci 30:15585–15599.

Moss J, Ungless MA, Bolam JP (2011) Dopaminergic axons in different divisions of the adult rat striatal complex do not express vesicular glutamate transporters. Eur J Neurosci 33:1205–1211.

Omelchenko N, Sesack SR (2005) Laterodorsal tegmental projections to identified cell populations in the rat ventral tegmental area. J Comp Neurol 483:217–235.

Omelchenko N, Bell R, Sesack SR (2009) Lateral habenula projections to dopamine and GABA neurons in the rat ventral tegmental area. Eur J Neurosci 30:1239–1250.

Petreanu L, Huber D, Sobczyk A, Svoboda K (2007) Channelrhodopsin-2-assisted circuit mapping of long-range callosal projections. Nat Neurosci 10:663–668.

Saal D, Dong Y, Bonci A, Malenka RC (2003) Drugs of abuse and stress trigger a common synaptic adaptation in dopamine neurons. Neuron 37:577–582.

Schmidt HD, Famous KR, Pierce RC (2009) The limbic circuitry underlying cocaine seeking encompasses the PPTg/LDT. Eur J Neurosci 30:1358–1369.

Sesack SR, Pickel VM (1992) Prefrontal cortical efferents in the rat synapse on unlabeled neuronal targets of catecholamine terminals in the nucleus accumbens septi and on dopamine neurons in the ventral tegmental area. J Comp Neurol 320:145–160.

Sparta DR, Stamatakis AM, Phillips JL, Hovelsø N, van Zessen R, Stuber GD (2011) Construction of implantable optical fibers for long-term optogenetic manipulations of neural circuits. Nat Protoc 7:12–23.

Stuber GD, Hopf FW, Hahn J, Cho SL, Guillory A, Bonci A (2008) Voluntary ethanol intake enhances excitatory synaptic strength in the ventral tegmental area. Alcohol Clin Exp Res 32:1714–1720.

Stuber GD, Hnasko TS, Britt JP, Edwards RH, Bonci A (2010) Dopaminergic terminals in the nucleus accumbens but not the dorsal striatum corelease glutamate. J Neurosci 30:8229–8233.

Stuber GD, Sparta DR, Stamatakis AM, van Leeuwen WA, Hardjoprajitno JE, Cho S, Tye KM, Kempadoo KA, Zhang F, Deisseroth K, Bonci A (2011) Excitatory transmission from the amygdala to nucleus accumbens facilitates reward seeking. Nature 475:377–380.

© 2013 Stuber

NOTES

Sulzer D, Joyce MP, Lin L, Geldwert D, Haber SN, Hattori T, Rayport S (1998) Dopamine neurons make glutamatergic synapses *in vitro*. J Neurosci 18:4588–4602.

Swanson LW (1982) The projections of the ventral tegmental area and adjacent regions: a combined fluorescent retrograde tracer and immunofluorescence study in the rat. Brain Res Bull 9:321–353.

Tecuapetla F, Patel JC, Xenias H, English D, Tadros I, Shah F, Berlin J, Deisseroth K, Rice ME, Tepper JM, Koos T (2010) Glutamatergic signaling by mesolimbic dopamine neurons in the nucleus accumbens. J Neurosci 30:7105–7110.

Tong ZY, Overton PG, Clark D (1996) Stimulation of the prefrontal cortex in the rat induces patterns of activity in midbrain dopaminergic neurons which resemble natural burst events. Synapse 22:195–208.

Tsai HC, Zhang F, Adamantidis A, Stuber GD, Bonci A, de Lecea L, Deisseroth K (2009) Phasic firing in dopaminergic neurons is sufficient for behavioral conditioning. Science 324:1080–1084.

Tye KM, Prakash R, Kim SY, Fenno LE, Grosenick L, Zarabi H, Thompson KR, Gradinaru V, Ramakrishnan C, Deisseroth K (2011) Amygdala circuitry mediating reversible and bidirectional control of anxiety. Nature 471:358–362.

Ungless MA, Whistler JL, Malenka RC, Bonci A (2001) Single cocaine exposure *in vivo* induces long-term potentiation in dopamine neurons. Nature 411:583–587.

Van Bockstaele EJ, Pickel VM (1995) GABA-containing neurons in the ventral tegmental area project to the nucleus accumbens in rat brain. Brain Res 682:215–221.

Wang H, Peca J, Matsuzaki M, Matsuzaki K, Noguchi J, Qiu L, Wang D, Zhang F, Boyden E, Deisseroth K, Kasai H, Hall WC, Feng G, Augustine GJ (2007) High-speed mapping of synaptic connectivity using photostimulation in Channelrhodopsin-2 transgenic mice. Proc Natl Acad Sci USA. 104:8143–8148.

Wise RA (2004) Dopamine, learning and motivation. Nat Rev Neurosci 5:483–494.

Witten IB, Steinberg EE, Lee SY, Davidson TJ, Zalocusky KA, Brodsky M, Yizhar O, Cho SL, Gong S, Ramakrishnan C, Stuber GD, Tye KM, Janak PH, Deisseroth K (2011) Recombinase-driver rat lines: tools, techniques, and optogenetic application to dopamine-mediated reinforcement. Neuron 72:721–733.

Xia Y, Driscoll JR, Wilbrecht L, Margolis EB, Fields HL, Hjelmstad GO (2011) Nucleus accumbens medium spiny neurons target non-dopaminergic neurons in the ventral tegmental area. J Neurosci 31:7811–7816.

Yizhar O, Fenno LE, Davidson TJ, Mogri M, Deisseroth K (2011) Optogenetics in neural systems. Neuron 71:9–34.

You ZB, Tzschentke TM, Brodin E, Wise RA (1998) Electrical stimulation of the prefrontal cortex increases cholecystokinin, glutamate, and dopamine release in the nucleus accumbens: an *in vivo* microdialysis study in freely moving rats. J Neurosci 18:6492–6500.

You ZB, Wang B, Zitzman D, Azari S, Wise RA (2007) A role for conditioned ventral tegmental glutamate release in cocaine seeking. J Neurosci 27:10546–10555.

Zhang F, Wang LP, Brauner M, Liewald JF, Kay K, Watzke N, Wood PG, Bamberg E, Nagel G, Gottschalk A, Deisseroth K (2007) Multimodal fast optical interrogation of neural circuitry. Nature 446:633–639.

Zhang F, Gradinaru V, Adamantidis AR, Durand R, Airan RD, de Lecea L, Deisseroth K (2010) Optogenetic interrogation of neural circuits: technology for probing mammalian brain structures. Nat Protoc 5:439-456.

Zhao S, Ting JT, Atallah HE, Qiu L, Tan J, Gloss B, Augustine GJ, Deisseroth K, Luo M, Graybiel AM, Feng G (2011) Cell type-specific channelrhodopsin-2 transgenic mice for optogenetic dissection of neural circuitry function. Nat Methods. 8:745–752.

© 2013 Stuber

Chemogenetic Inhibition of Serotonergic Neurons Reveals Their Key Role in Physiological Homeostasis

Russell Ray, PhD,[1,5] Andrea Corcoran, PhD,[2] Rachael Brust, BS,[1] Jun Chul Kim, PhD,[3] George B. Richerson, MD, PhD,[4] Eugene Nattie, MD, PhD,[2] and Susan M. Dymecki, MD, PhD[1]

[1]Department of Genetics
Harvard Medical School
Boston, Massachusetts

[2]Department of Physiology
Dartmouth Medical School
Lebanon, New Hampshire

[3]Department of Psychology
University of Toronto
Toronto, Ontario, Canada

[4]Department of Neurology
University of Iowa Hospitals and Clinics
Iowa City, Iowa

[5]Department of Neuroscience
Center on Addiction, Learning, and Memory
Baylor College of Medicine
Houston, Texas

© 2013 Dymecki

NOTES

Introduction: Serotonergic Involvement in Homeostasis

Normal mammalian cell and organism function requires relative constancy around optimal internal physiological conditions. Maintaining this dynamic equilibrium involves neuronal networks affecting numerous brain and body systems. One such homeostatic reflex, the respiratory chemoreflex, controls ventilation in response to deviations in arterial and brainstem pH/PCO_2 (partial pressure of CO2) (Haldane and Priestley, 1905; Leusen, 1954; Kety and Forster, 2001; Smith et al., 2006; Guyenet et al., 2010; Nattie, 2011). Various classes of brainstem cells (Mitchell et al., 1963; Elam et al., 1981; Williams et al., 2007; Li et al., 2008; Gourine et al., 2010; Nattie, 2011) have been implicated, and integration and redundancy among components have been found to be likely essential. Serotonergic neurons of the lower brainstem have been proposed as one critical constituent (Richerson, 1995; Wang and Richerson, 1999; Corcoran et al., 2009; Hodges and Richerson, 2010; Depuy et al., 2011; Nattie, 2011). These neurons also have been implicated in other homeostatic circuitry, such as the thermoregulatory network for maintaining body temperature (Cano et al., 2003; Hodges et al., 2008; Morrison et al., 2008). Fatal or life-threatening clinical disorders of homeostatic dysfunction also point to serotonergic involvement, as in the sudden infant death syndrome (SIDS) (Kinney et al., 2009; Duncan et al., 2010) and serotonin syndrome (Sternbach, 1991). Direct evidence demonstrating a requirement for serotonergic neurons in homeostasis, however, is only now emerging (Hodges et al., 2008; Depuy et al., 2011) as tools with sufficient resolving power become available.

A Genetic Tool for Suppressing Neuronal Excitability

To test whether serotonergic neuron activity is critical to homeostatic control, we engineered a genetic tool, allele *RC::FPDi* (Fig. 1A), for suppressing neuronal excitability in conscious mice inducibly, reversibly, with cell-subtype precision, and with minimal invasiveness. We used conditional intersectional genetics (Awatramani et al., 2003; Jensen et al., 2008; Kim et al., 2009) to switch on the expression of the synthetic receptor Di (DREADD, hM_4D) (Armbruster et al., 2007, in which DREADD stands for "designer receptors exclusively activated by designer drug"). This $G_{i/o}$-protein coupled receptor (GPCR) offers engineered selectivity for the biologically inert synthetic ligand clozapine-*N*-oxide (CNO) while being refractive to

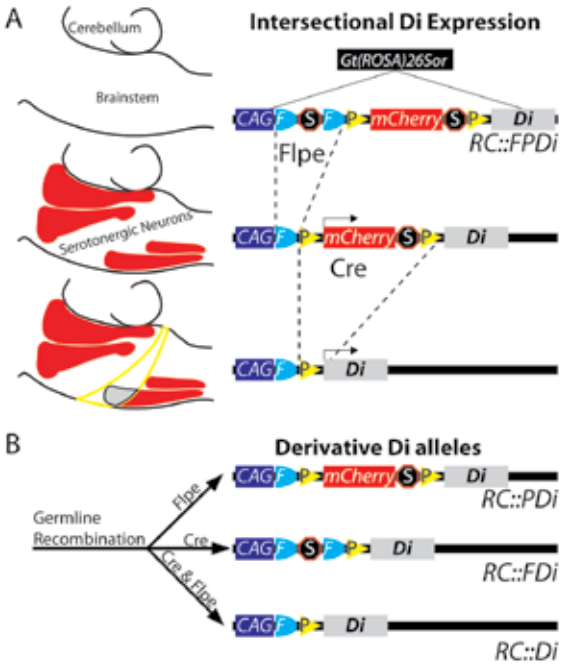

Figure 1. Cell-selective Di expression via *RC::FPDi*. *A,* This *Gt(ROSA)26Sor* knock-in allele consists of *CAG* regulatory elements, an *FRT*-flanked transcriptional Stop, a *lox*P-flanked mCherry-Stop, and HA-tagged-Di-encoding sequence. A hypothetical example (left) illustrates intersectional restriction of Di to a serotonergic neuron subset (gray area, lower schema) after Flpe and Cre recombination; mCherry marks Flpe-only cells (red areas represent serotonergic nuclei); neither Di nor mCherry are expressed in Cre-only cells (yellow circumscribed area). ***B,*** Derivative Di alleles.

endogenous ligands. Like endogenous $G_{i/o}$-GPCRs, the binding of CNO by Di has been shown capable of triggering cell-autonomous hyperpolarization and diminished cell excitability (Mark and Herlitze, 2000; Armbruster et al., 2007; Ferguson et al., 2011). Our tool, *RC::FPDi*, a knock-in *ROSA26* allele utilizing the CAG promoter (Dymecki and Kim, 2007), offers nonviral means of Di expression. It exploits the dual-recombinase methodology that endows Cre and Flpe transgenics with the potential to switch on Di expression in combinatorially defined neuron subtypes, as previously demonstrated for various intersectional alleles (Awatramani et al., 2003; Jensen et al., 2008; Kim et al., 2009).

To meet the needs for single recombinase-mediated Di expression (versus the dual-recombinase strategy), we generated derivatives of *RC::FPDi* (Fig. 1*B*): *RC::PDi* requires only Cre to switch on Di expression because the *FRT*-cassette was excised in the ancestral germline; reciprocally, *RC::FDi*

© 2013 Dymecki

NOTES

requires only Flpe to switch on Di expression. By partnering *RC::PDi* with *Slc6a4-cre*, we expressed Di in virtually all serotonergic neurons and a small subset of thalamic neurons. We also incorporated a Cre-responsive GFP allele, *RC::rePe*, to fluorescently visualize the *Slc6a4-cre* lineage, thereby facilitating validation of lineage-specific Di expression as well as the electrophysiological study of Di-expressing neurons (Fig. 2).

Modulating Serotonergic Neuron Activity

To test Di in modulating serotonergic neuron activity, as driven by *RC::PDi*, we made current–clamp membrane potential recordings (Fig. 2) from lower brainstem serotonergic neurons cultured from *RC::PDi; Slc6a4-cre* mice. Once again, these were coupled with *RC:rePe* to fluorescently identify Cre-expressing, and thus, Di-expressing neurons. CNO reduced the firing rate of Di-expressing neurons by ~40% on average (Fig. 2*D*). This reduction was similar to that successively observed in the same neurons following application of 8-OH-DPAT (Figs. 2*C, D*). 8-OH-DPAT is an agonist for the endogenous inhibitory serotonin autoreceptor $5HT_{1A}$, which is a GPCR known to act through $G_{i/o}$ and Kir3 channels to inhibit serotonergic neuron excitability (Penington et al., 1993; Mark and Herlitze, 2000).

The response onset to CNO occurred on average 1.3 ± 0.1 (SEM) min after switching the perfusion port from artificial cerebrospinal fluid (aCSF) to CNO, with bath superfusate exchange taking ~1 min, suggesting response onset within seconds. Peak responses to CNO occurred 2.8 ± 0.3 (SEM) min after port switching, thus, within ~2 min of CNO exposure. The CNO-induced suppression of action potential firing reversed on return to control superfusate (Figs. 2*A–D*). This reversal reached full recovery on average in 12.4 ± 2.9 (SEM) min (though with notable variation from 0.9 to 25.4 min), loosely correlating with duration of CNO exposure. The CNO-induced suppression could be blocked by the potassium-channel inhibitor barium chloride (300 μM) (Figs. 2*E, F*), consistent with a Kir3 mechanism of neuron inhibition. Neuron-to-neuron variation in firing-rate suppression occurred not only in response to CNO (0.58 ± 0.07 [SEM], normalized to baseline values pre-CNO) (Fig. 2*D*) but also to 8-OH-DPAT (0.37 ± 0.09 [SEM]), likely reflecting endogenous heterogeneity among 5-HT neuron subtypes. That is, not all serotonergic neurons express $5HT_{1A}$ autoreceptors (Bonnavion et al., 2010), nor may they all express Kir3-type channels.

The current–voltage relationships characterizing Di-expressing serotonergic neurons revealed activation, by CNO/Di, of an inwardly rectifying conductance reversing near the predicted reversal potential for potassium (predicted E_K = –81 mV; measured E_K = –78 ± 1.9 [SEM] mV) (Fig. 2G). Responsive neurons (8 of 17 in this assay) demonstrated an increase in slope conductance averaging 2.7 ± 1.1 (SEM) pS between –110 and –90 mV, and a hyperpolarizing current of 16 ± 3.6 (SEM) pA at –60 mV (Fig. 2*H*), ranging between 5 and 45 pA across potentials of –60 to –50 mV. This resting-potential range included most serotonergic neurons (Wang, Pizzonia et al., 1998; Wang and Richerson, 1999). The response to 8-OH-DPAT in the same neurons was similar: hyperpolarizing currents of 17.7 ± 4.7 (SEM) pA at –60 mV ranged between 5 and 85 pA across –50 to –60 mV, and slope conductance increased by 4.7 ± 1.3 (SEM) pS between –110 and –90 mV. Control serotonergic neurons (Figs. 2*D, H*) exhibited a similarly robust response to 8-OH-DPAT but not to CNO; this difference indicates that CNO in the absence of Di does not measurably affect membrane conductance or action potential firing rate. Collectively, these findings point to CNO/Di, like 8-OH-DPAT and the $5HT_{1A}$ autoreceptor, evoking hyperpolarizing outward potassium currents via Kir3-type channels.

Assessing serotonergic neuron activity in the respiratory chemoreflex

Hypercapnic acidosis (a decrease in tissue pH caused by PCO_2 elevation from ventilatory dysfunction or cellular metabolism) is a powerful respiratory stimulus. To assess the requirement for serotonergic neuron activity in the CO_2-driven respiratory chemoreflex, we measured the ventilatory response of adult *RC::PDi; Slc6a4-cre* mice and sibling controls to an increase in inspired CO_2 from 0% (room air) to 5% (a modest rise) before and after CNO injection (Figs. 3A–C). The typical increase in ventilation for restoring normal arterial pH/PCO_2 levels was reduced by ~50% in *RC::PDi; Slc6a4-cre* mice within minutes following CNO administration (Fig. 3*B*). Prior to CNO, CO_2 exposure had evoked a ventilatory response comparable with that seen in control siblings, indicating that Di expression alone does not affect the chemoreflex. Nor is CNO alone inhibitory, given the normal ventilatory response of CNO-treated control siblings (Fig. 3C). We obtained similar results when the *Slc6a4-cre* driver was replaced with *Pet1::Flpe* (Jensen et al., 2008), an alternative serotonergic neuron driver, and partnered with *RC::FDi*. In this way, we independently confirmed attribution of function to serotonergic neurons.

© 2013 Dymecki

NOTES

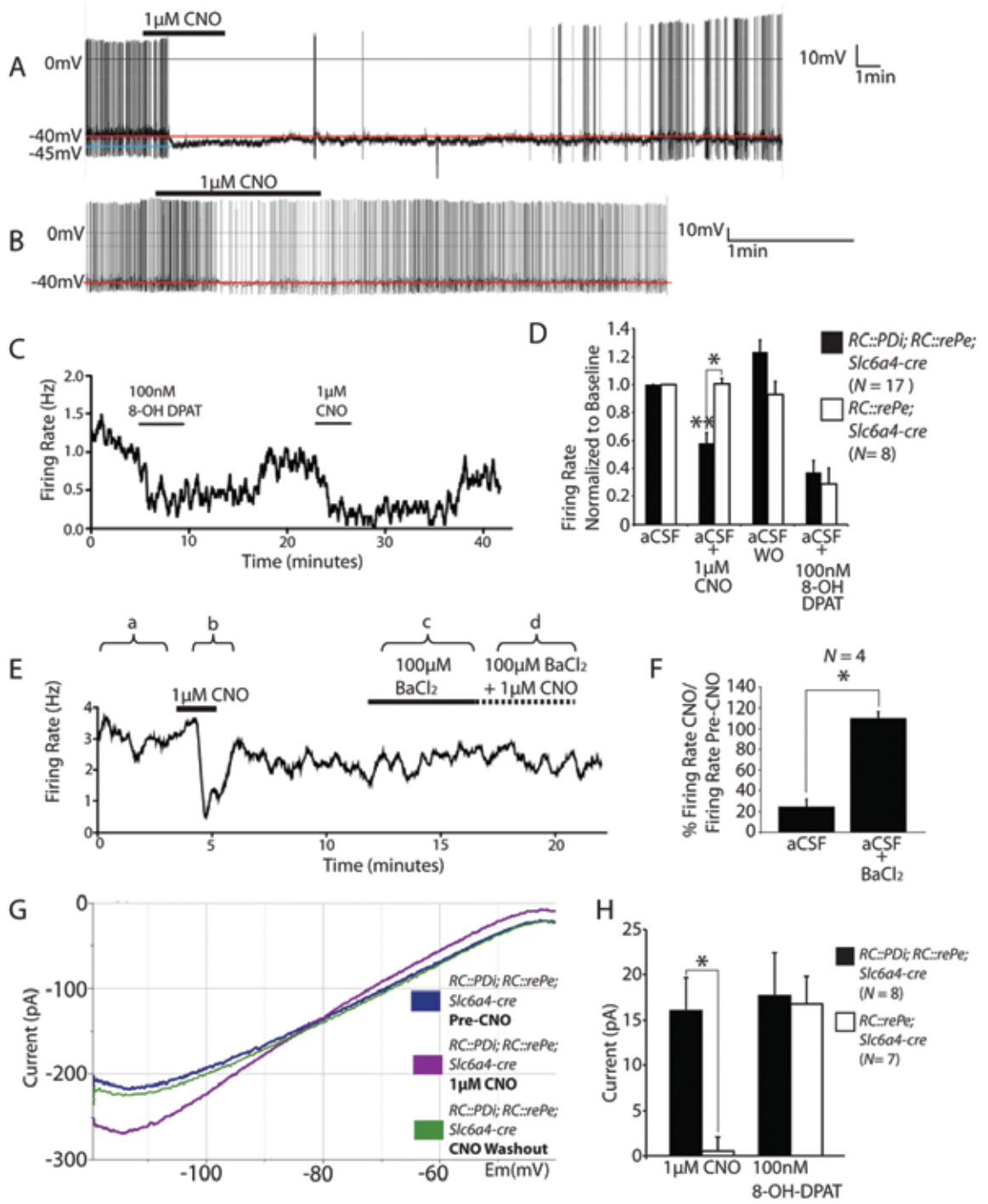

Figure 2. Inducible and reversible suppression of serotonergic neuron excitability using *RC::PDi*. ***A, B,*** Recordings of cultured medullary serotonergic neurons from *RC::PDi; RC::rePe; Slc6a4-cre* mice showing CNO-induced abolishment *(A)* or moderate suppression *(B)* of action potential firing, with recovery following return to aCSF superfusate. ***C,*** Firing rate during sequential applications of 8-OH-DPAT and CNO. ***D,*** Average firing rates (normalized to baseline ± SEM) of Di/green fluorescent protein (GFP)–expressing versus control neurons. Inhibition by CNO was observed for Di neurons compared with pre-CNO, post-CNO aCSF superfusate (aCSF washout [WO] of CNO), and CNO-exposed control neurons; $^{**}p < 0.0001$ (Friedman test); $^{*}p < 0.005$ (Mann–Whitney *U* test). CNO-inhibition was comparable with that of 8-OH-DPAT (*n = 9 RC::PDi; RC::rePe; Slc6a4-cre* neurons; *n = 8 control neurons*). ***E,*** Sample trace of $BaCl_2$-mediated block of CNO-induced suppression. ***F,*** Average ratio of firing rate for CNO versus pre-CNO, expressed as a percentage ± SEM. Neurons were assayed in aCSF (*a* and *b* in *E*) and upon subsequent application of B_aCl_2 (*c* and *d*); $^{*}p < 0.05$ (Friedman test). ***G,*** Voltage-clamp recording showing the current–voltage relationship of a Di-expressing serotonergic neuron with or without CNO. ***H,*** Average current elicited by CNO and 8-OH-DPAT at –60 mV; $^{*}p = 0.002$ (Mann–Whitney *U* test). Calibrations: ***A, B,*** 1 µM (CNO); ***C***, 100 nM (8-OH-DPAT); ***E,*** 1 µM (CNO); 100 µM ($BaCl_2$).

© 2013 Dymecki

NOTES

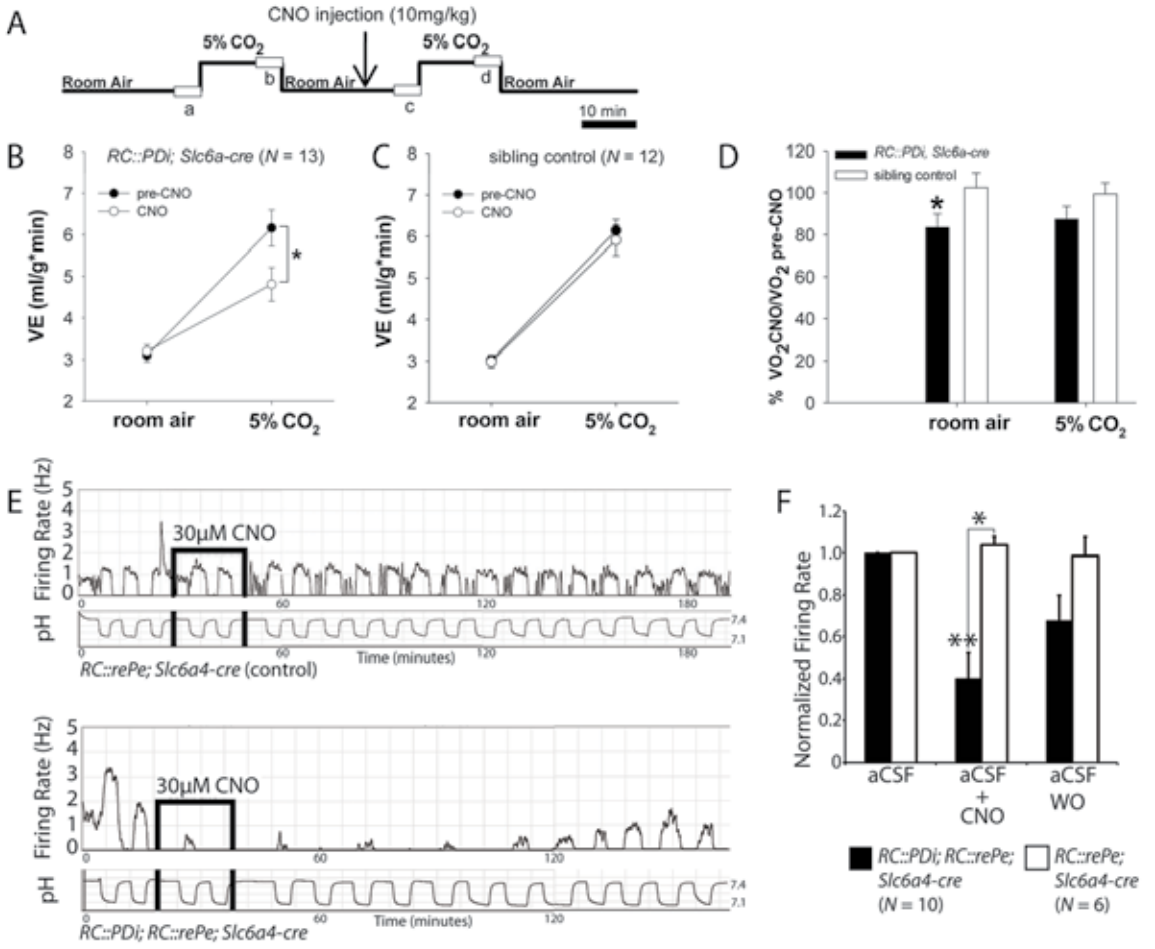

Figure 3. CNO/Di perturbation of serotonergic neurons disrupts the central respiratory CO_2 chemoreflex. ***A,*** Protocol for plethysmographic assessment at 34°C of respiratory responses to inspired CO_2 in the awake animal before and after CNO administration. Boxes *a, b, c,* and *d* represent points analyzed from continuous recordings. ***B,*** *RC::PDi; Slc6a4-cre* mice upon CNO administration showed reduced-minute ventilation responses to inspired CO_2 compared with pre-CNO baselines; $^*p = 0.002$ (repeated-measures [RM] ANOVA followed by Tukey's test). ***C,*** Pre-CNO and CNO responses to CO_2 were indistinguishable for control mice and from the pre-CNO response of *RC::PDi; Slc6a4-cre* mice. ***D,*** *RC::PDi; Slc6a4-cre* mice exhibited reduced VO_2 upon CNO administration compared with controls; $^*p < 0.05$ (paired *t* test). ***E,*** Firing rate and simultaneous bath pH recordings from cultured sarotonergic neurons from controls (top) compared with *RC::PDi; RC::rePe; Slc6a4-cre* mice (bottom). Changing CO_2 from 5% to 9% shifted pH from ~7.4 to ~7.16 and induced an increase in firing rate. In Di neurons (bottom), this response was inhibited by CNO and reversed on return to aCSF. ***F,*** Peak firing rates (normalized to baseline) in 9% CO_2-saturated aCSF were suppressed with CNO application in *RC::PDi; RC::rePe; Slc6a4-cre* neurons; $^*p < 0.05$ (Mann–Whitney *U* test).

Room air ventilation was unaffected following CNO/Di manipulation of *Slc6a4-cre*-expressing neurons (Figs. 3*A–D*). This phenomenon is reminiscent of phenotypes reported for adult mice in which embryonic deletion of the gene *lmx1b* in Pet1-expressing cells results in developmental loss of most if not all serotonergic neurons (Hodges et al., 2008). Notably, following CNO injection, oxygen consumption in room air dropped from within- to below-normal range (0.053 ± 0.003[SEM] ml/g/min to 0.043 ± 0.003[SEM] ml/g/min) in *RC::PDi; Slc6a4-cre* mice but not in controls (Fig. 3*D*). Thus, Di-mediated perturbation of *Slc6a4-cre*-expressing neurons led to a decrease in metabolic rate without proportionately matching effects on ventilation. An additional role for serotonergic neurons may thus be supported: that of influencing metabolic rate and the ability of ventilation to properly track with metabolic state.

Triggering the chemoreflex requires sensing and transducing milieu changes in pH/PCO_2 into

© 2013 Dymecki

NOTES

cellular activity changes, e.g., in action potential firing rates capable of affecting respiratory circuit output and breathing. We found that cultured serotonergic neurons from the lower brainstem reproducibly increased their firing rate 2- to 3-fold in response to acidosis (0.2–0.3 pH units, a magnitude of physiological relevance) caused by increasing the CO_2 bubbled in the superfusate from 5% to 9% (Fig. 3*E*). This finding is consistent with previous ones in serotonergic neurons from rats (Richerson, 1995; Wang and Richerson, 1999). Approximately 70% of medullary serotonergic neurons exhibit chemosensitivity, supporting the view that not all medullary serotonergic neurons project to brainstem respiratory centers; rather, this property likely distinguishes a specific functional subset of serotonergic neurons.

Because we performed recordings under conditions of relative synaptic isolation (blockade of $GABA_A$, NMDA, and AMPA/kainate receptors by picrotoxin, AP5, and CNQX, respectively), the observed chemosensitivity may be an intrinsic property of these serotonergic neurons. CNO administration inhibited this chemoresponsiveness (1 μM CNO [data not shown] or 30 μM CNO [Figs. 3*E*, *F*]) at concentrations less than or comparable with that delivered *in vivo*, which could be restored upon return to control superfusate. Control, non–Di-expressing serotonergic neurons showed no response to CNO (Fig. 3*E*, upper panel). CNO was continuously applied over 2–3 pH cycles for an average of 20 min (versus the ~5 min exposure during firing rate assays) (Figs. 2*A–D*). Recovery times were longer (76.3 ± 60.7 [SEM] min) following this extended CNO exposure.

These data support the parsimonious model whereby a subset of serotonergic neurons in the lower brainstem acts as central respiratory chemoreceptors capable of regulating the downstream respiratory network (and thus, lung ventilation) in an attempt to restore normal arterial pH/PCO_2 (Dias et al., 2008; Hodges et al., 2008; Corcoran et al., 2009; Hodges and Richerson, 2010; Nattie, 2011). PCO_2 stabilization is also served by Phox2B-expressing glutamatergic neurons of the brainstem retrotrapezoid nucleus (Dubreuil et al., 2009; Marina et al., 2010). It will be important to determine how these and likely other (Mitchell et al., 1963; Elam et al., 1981; Williams et al., 2007; Marina et al., 2010; Nattie, 2011) neural systems integrate to control breathing, and under what developmental stages, arousal states, and conditions they may be differentially employed. Astrocytes along the brainstem surface have also been implicated as respiratory chemosensors capable of influencing retrotrapezoid neuron activity (Gourine et al., 2010; Wenker et al., 2010). So it will be important to assess whether astrocytes also influence serotonergic neurons and whether their effects on chemoreception persist in conscious animals.

Assessing serotonergic neuron activity in body temperature change

During the whole-body plethysmography (Fig. 3), chamber temperature was held at ~34°C to reduce effects of body temperature fluctuations on respiratory parameters and oxygen consumption. Under these conditions, core body temperature remained within ± 0.65°C (SEM) of baseline for controls and Di mice. Absent this thermoneutral environment, double-transgenic *RC::PDi; Slc6a4-cre* mice's body temperature dropped within minutes of CNO administration. While housed individually at room temperature (~23°C), *RC::PDi; Slc6a4-cre* mice's body temperature dropped from 36.9 ± 0.2°C (SEM) to 30.33 ± 0.2°C (SEM) within 30 min of CNO injection, dipping to 27.1 ± 0.9°C (SEM) by ~2.5 h (Fig. 4*A*). After this time, recovery ensued, with restoration to within normal range by 11.8 ± 1.3 h (SEM). Sibling controls receiving CNO showed normal thermoregulation (37.2 ± 0.03°C [SEM]).

These findings establish that *Slc6a4-cre*–expressing neuron activity is required for adult thermal homeostasis and that most thermoregulatory capacity is lost, given the near equilibration of body temperature to ambient room temperature. The kinetics of body temperature change (Fig. 4*A*) reflect, to a large degree, body thermal inertia, contrasting with the more rapid response observed for individual neurons (Fig. 2). Similar body temperature dysregulation was observed on replacing *Slc6a4-cre; RC::PDi* with *Pet1::Flpe; RC::FDi* (data not shown), thereby independently confirming attribution of function to serotonergic neurons. (Note, however, that in the latter case, the extent of temperature dysregulation is less severe, likely because the *Pet1::Flpe* driver shows mosaicism in recombinase expression in medullary serotonergic neurons.) Delineating the effectors of body temperature homeostasis acting downstream of serotonergic circuitry will be an important next step.

In contrast to the response evoked upon acute serotonergic neuron inhibition, adult mice devoid of serotonin-producing neurons from midgestation onward are able to maintain a near wild-type body temperature (~36°–38°C) while housed at room temperature (~24°C) (Hodges et al., 2008; Hodges

© 2013 Dymecki

NOTES

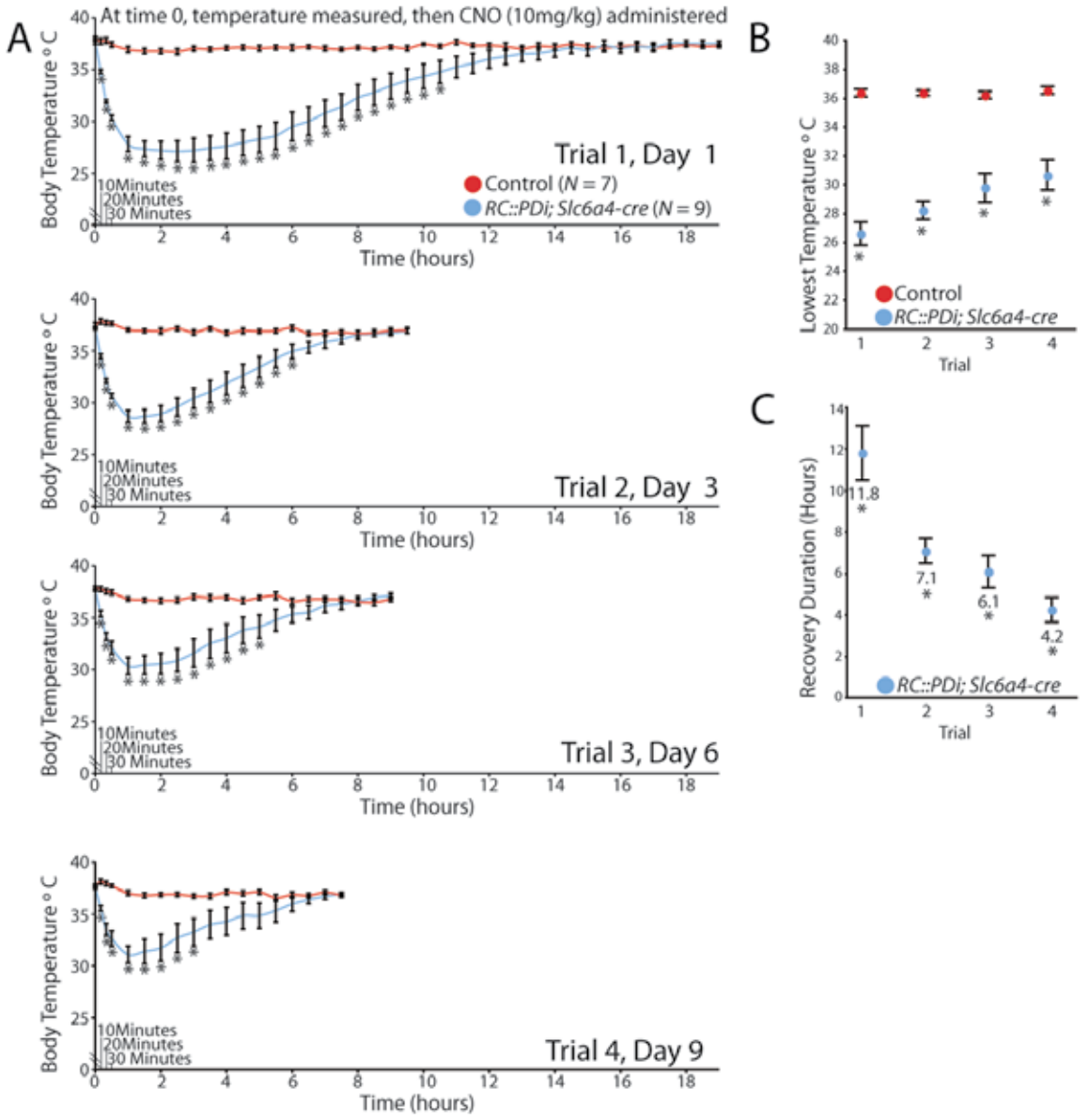

Figure 4. CNO/Di inhibition of serotonergic neurons induced severe yet reversible and repeatable hypothermia. Trials consisted of body temperature assessments taken at room temperature just before a single CNO administration and then every 10 min for the first one-half hour, followed by every 30 min until recovery. Animals underwent 4 sequential trials. ***A,*** Body temperature averages of *RC::PDi; Slc6a4-cre* mice versus controls before and after CNO injection; *$p < 0.05$ (unpaired *t* test). ***B,*** Average lowest temperatures achieved per trial; *$p < 0.05$ (a one-way RM ANOVA). ***C,*** Average duration to return to 36°C following CNO injection; *$p < 0.01$ (a one-way RM ANOVA).

and Richerson, 2010). This phenotypic difference indicates that compensatory circuitry arises in the face of developmental loss of serotonergic neurons. It also highlights how acute neuron perturbation avoids such confounds.

Repeated neuron perturbation in the same animal is possible: With each round of CNO administration, body temperature plummeted within minutes (Fig. 4A). The severity of the induced hypothermia, though, showed adaptation with each subsequent trial (Fig. 4B); also, the time required for return to baseline body temperature showed adaptation (Fig. 4C). We observed no overt behavioral deficits (short- or long-term) following these bouts of CNO/Di-triggered hypothermia, perhaps not surprising, given rodents' capacity for daily torpor.

© 2013 Dymecki

NOTES

Implications: Serotonin Abnormalities in SIDS and Other Syndromes

Using this *RC::FPDi* strategy, we have revealed impaired respiratory and body temperature control upon acute perturbation of serotonergic neuron activity. These results provide direct evidence that serotonergic neurons play key roles in the central chemoreflex and thermoregulation. These findings offer potential mechanistic explanation for fatal or life-threatening disorders of homeostasis that are associated with serotonin abnormalities, such as SIDS and the serotonin syndrome.

In SIDS, the leading cause of death in children between 1 month and 1 year of age (Kinney et al., 2009), multiple abnormalities in the brainstem serotonergic system have been identified, including serotonin insufficiency (Kinney et al., 2009; Duncan et al., 2010). Our findings suggest that such insufficiency might compromise an infant's respiratory response to hypercapnic acidosis, which may occur upon rebreathing exhaled air as a result of sleeping prone, in the face-down position (SIDS infants are often found prone), contributing to respiratory failure and death. By contrast, serotonin syndrome is a disorder of serotonin excess and extreme hyperthermia, shivering, seizures, coma, and in some cases, death that can result acutely from serotonin drug interactions (Sternbach, 1991). This association between serotonin excess and hyperthermia is consistent with our reciprocal findings of serotonergic inhibition inducing hypothermia.

We presume that *in vivo*, CNO/Di signaling suppresses action potential firing, resulting in net inhibition of serotonergic neuron activity (Innis and Aghajanian, 1987; Pineyro and Blier, 1999). Other scenarios are possible, such as net excitation, but seem improbable owing to the whole-animal phenotypes observed upon CNO/Di signaling in serotonergic neurons, the molecular mechanism by which Di appears to act, and the paucity of evidence that net excitation could occur. For example, such net excitation has not been observed in cultured serotonergic neurons nor in extensive studies on $5HT_{1A}$ receptor agonists, either *in vivo* or *ex vivo*, which act mechanistically like CNO/Di (Innis and Aghajanian, 1987; Pineyro and Blier, 1999).

Conclusion

Assessing the precise *in vivo* electrophysiological consequences of CNO/Di signaling on serotonergic neuron activity, including chemoresponsiveness, awaits the means to record from individual medullary serotonergic neurons over the course of hours (compare Fig. 3*E*) in unanesthetized, conscious mice. By contrast, recordings under either anesthesia (Patel et al., 1999; Gobbi et al., 2007; Depuy et al., 2011) or decerebration (Hayashi and Sinclair, 1991; St-John and Paton, 2000) suffer from the confound of perturbing serotonergic neuron activity and chemoreflex properties—the very processes under examination.

The present studies, as well as our analyses of broad constitutive Di expression and activity, establish *RC::FPDi* as a neuronal perturbation tool. This tool features *in vivo* ligand inducibility within seconds to minutes, inhibition for minutes to hours, reversibility within hours, intra-animal repeatability, and high cell-subtype selectivity, and thus resolution, for functional mapping. It can be applied in the awake, freely behaving animal without adding confounding interference from anesthesia, surgical procedures (e.g., cannulation or intracranial fiber optics), or compensatory changes in circuitry that can develop in response to constitutive genetic alterations. *RC::FPDi* can be applied to map other behaviors in which dysregulation of specific populations has been implicated.

Acknowledgments

This work was supported by the following National Institutes of Health grants: F32HD063257-01A1 (R.R.); 5R21DA023643-02 (R.B., S.D.); 5R21MH083613-02 (R.R., J.C.K., S.D.); 5P01HD036379-13 (R.R., A.C., R.B., J.C.K., E.N., G.R., S.D.); 5R01HL028066-30 (A.C., E.N.); and 5R01HD052772 (G.R.). We wish to thank Bryan Roth for providing the Di-encoding cDNA, and Drs. Bryan Roth, Wade Regehr, Court Hull, and Bernardo Sabatini and Dymecki lab members for helpful discussions; and Yuanming Wu and Jia Jia Mai for their technical assistance. This chapter was adapted from an article published in the journal *Science:* Ray RS, Corcoran AE, Brust RD, et al. Impaired respiratory and body temperature control upon acute serotonergic neuron inhibition. 2011;333(6042):637–642.

© 2013 Dymecki

NOTES

References

Armbruster BN, Li X, Pausch MH, Herlitze S, Roth BL (2007) Evolving the lock to fit the key to create a family of G protein-coupled receptors potently activated by an inert ligand. Proc Natl Acad Sci USA 104:5163–5168.

Awatramani R, Soriano P, Rodriguez C, Mai JJ, Dymecki SM (2003) Cryptic boundaries in roof plate and choroid plexus identified by intersectional gene activation. Nat Genet 35:70–75.

Bonnavion P, Bernard JF, Hamon M, Adrien J, Fabre V (2010). Heterogeneous distribution of the serotonin 5-HT(1A) receptor mRNA in chemically identified neurons of the mouse rostral brainstem: implications for the role of serotonin in the regulation of wakefulness and REM sleep. J Comp Neurol 518:2744–2770.

Cano G, Passerin AM, Schiltz JC, Card JP, Morrison SF, Sved AF (2003) Anatomical substrates for the central control of sympathetic outflow to interscapular adipose tissue during cold exposure. J Comp Neurol 460:303–326.

Corcoran AE, Hodges MR, Wu Y, Wang W, Wylie CJ, Deneris ES, Richerson GB (2009) Medullary serotonin neurons and central CO2 chemoreception. Respir Physiol Neurobiol 168:49–58.

Depuy SD, Kanbar R, Coates MB, Stornetta RL, Guyenet PG (2011) Control of breathing by raphe obscurus serotonergic neurons in mice. J Neurosci 31:1981–1990.

Dias MB, Li A, Nattie E (2008) Focal CO_2 dialysis in raphe obscurus does not stimulate ventilation but enhances the response to focal CO_2 dialysis in the retrotrapezoid nucleus. J Appl Physiol 105:83–90.

Dubreuil V, Thoby-Brisson M, Rallu M, Persson K, Pattyn A, Birchmeier C, Brunet JF, Fortin G, Goridis C (2009) Defective respiratory rhythmogenesis and loss of central chemosensitivity in Phox2b mutants targeting retrotrapezoid nucleus neurons. J Neurosci 29:14836–14846.

Duncan JR, Paterson DS, Hoffman JM, Mokler DJ, Borenstein NS, Belliveau RA, Krous HF, Haas EA, Stanley C, Nattie EE, Trachtenberg FL, Kinney HC (2010) Brainstem serotonergic deficiency in sudden infant death syndrome. JAMA 303:430–437.

Dymecki SM, Kim JC (2007) Molecular neuroanatomy's "Three Gs": a primer. Neuron 54:17–34.

Elam M, Yao T, Thorén P, Svensson TH (1981) Hypercapnia and hypoxia: chemoreceptor-mediated control of locus coeruleus neurons and splanchnic, sympathetic nerves. Brain Res 222:373–381.

Ferguson SM, Eskenazi D, Ishikawa M, Wanat MJ, Phillips PE, Dong Y, Roth BL, Neumaier JF (2011) Transient neuronal inhibition reveals opposing roles of indirect and direct pathways in sensitization. Nat Neurosci 14:22–24.

Gobbi G, Cassano T, Radja F, Morgese MG, Cuomo V, Santarelli L, Hen R, Blier P (2007) Neurokinin 1 receptor antagonism requires norepinephrine to increase serotonin function. Eur Neuropsychopharmacol 17:328–338.

Gourine AV, Kasymov V, Marina N, Tang F, Figueiredo MF, Lane S, Teschemacher AG, Spyer KM, Deisseroth K, Kasparov S (2010) Astrocytes control breathing through pH-dependent release of ATP. Science 329:571–575.

Guyenet PG, Stornetta RL, Bayliss DA (2010) Central respiratory chemoreception. J Comp Neurol 518:3883–3906.

Haldane JS, Priestley JG (1905) The regulation of the lung-ventilation. J Physiol 32:225–266.

Hayashi F, Sinclair JD (1991) Respiratory patterns in anesthetised rats before and after anemic decerebration. Respir Physiol 84:61–76.

Hodges MR, Richerson GB (2010) The role of medullary serotonin (5-HT) neurons in respiratory control: contributions to eupneic ventilation, CO_2 chemoreception, and thermoregulation. J Appl Physiol 108:1425–1432.

Hodges MR, Tattersall GJ, Harris MB, McEvoy SD, Richerson DN, Deneris ES, Johnson RL, Chen ZF, Richerson GB (2008) Defects in breathing and thermoregulation in mice with near-complete absence of central serotonin neurons. J Neurosci 28:2495–2505.

Innis RB, Aghajanian GK (1987) Pertussis toxin blocks 5-HT_{1A} and $GABA_B$ receptor-mediated inhibition of serotonergic neurons. Eur J Pharmacol 143:195–204.

Jensen P, Farago AF, Awatramani RB, Scott MM, Deneris ES, Dymecki SM (2008) Redefining the serotonergic system by genetic lineage. Nat Neurosci 11:417–419.

Kety SS, Forster RE (2001) Julius H. Comroe, Jr.: March 13, 1911–July 31, 1984. Biogr Mem Natl Acad Sci 79:66–83.

© 2013 Dymecki

NOTES

Kim JC, Cook MN, Carey MR, Shen C, Regehr WG, Dymecki SM (2009) Linking genetically defined neurons to behavior through a broadly applicable silencing allele. Neuron 63:305–315.

Kinney HC, Richerson GB, Dymecki SM, Darnall RA, Nattie EE (2009) The brainstem and serotonin in the sudden infant death syndrome. Annu Rev Pathol 4:517–550.

Leusen IR (1954) Chemosensitivity of the respiratory center; influence of CO_2 in the cerebral ventricles on respiration. Am J Physiol 176:39–44.

Li A, Emond L, Nattie E (2008) Brainstem catecholaminergic neurons modulate both respiratory and cardiovascular function. Adv Exp Med Biol 605:371–376.

Marina N, Abdala AP, Trapp S, Li A, Nattie EE, Hewinson J, Smith JC, Paton JF, Gourine AV (2010) Essential role of Phox2b-expressing ventrolateral brainstem neurons in the chemosensory control of inspiration and expiration. J Neurosci 30:12466–12473.

Mark MD, Herlitze S (2000) G-protein mediated gating of inward-rectifier K^+ channels. Eur J Biochem 267:5830–5836.

Mitchell RA, Loeschcke HH, Massion WH, Severinghaus JW (1963) Respiratory responses mediated through superficial chemosensitive areas on the medulla. J Appl Physiol 18:523–533.

Morrison SF, Nakamura K, Madden CJ (2008) Central control of thermogenesis in mammals. Exp Physiol 93:773–797.

Nattie E (2011) Julius H. Comroe, Jr., distinguished lecture: central chemoreception: then ... and now. J Appl Physiol 110:1–8.

Patel AJ, Honoré E, Lesage F, Fink M, Romey G, Lazdunski M (1999) Inhalational anesthetics activate two-pore-domain background K^+ channels. Nat Neurosci 2:422–426.

Penington NJ, Kelly JS, Fox AP (1993) Whole-cell recordings of inwardly rectifying K^+ currents activated by 5-HT_{1A} receptors on dorsal raphe neurones of the adult rat. J Physiol 469:387–405.

Pineyro G, Blier P (1999) Autoregulation of serotonin neurons: role in antidepressant drug action. Pharmacol Rev 51:533–591.

Richerson GB (1995) Response to CO_2 of neurons in the rostral ventral medulla *in vitro*. J Neurophysiol 73:933–944.

Smith CA, Rodman JR, Chenuel BJ, Henderson KS, Dempsey JA (2006) Response time and sensitivity of the ventilatory response to CO_2 in unanesthetized intact dogs: central vs. peripheral chemoreceptors. J Appl Physiol 100:13–19.

St-John WM, Paton JF (2000) Characterizations of eupnea, apneusis and gasping in a perfused rat preparation. Respir Physiol 123:201–213.

Sternbach H (1991) The serotonin syndrome. Am J Psychiatry 148:705–713.

Wang W, Pizzonia JH, Richerson GB (1998) Chemosensitivity of rat medullary raphe neurones in primary tissue culture. J Physiol 511(Pt 2):433–450.

Wang W, Richerson GB (1999) Development of chemosensitivity of rat medullary raphe neurons. Neuroscience 90:1001–1011.

Wenker IC, Kréneisz O, Nishiyama A, Mulkey DK (2010) Astrocytes in the retrotrapezoid nucleus sense H^+ by inhibition of a Kir4.1-Kir5.1-like current and may contribute to chemoreception by a purinergic mechanism. J Neurophysiol 104:3042–3052.

Williams RH, Jensen LT, Verkhratsky A, Fugger L, Burdakov D (2007) Control of hypothalamic orexin neurons by acid and CO_2. Proc Natl Acad Sci USA 104:10685–10690.

© 2013 Dymecki

Wireless Optogenetics

Jordan G. McCall, MPH, Tae-il Kim, PhD, Gunchul Shin, PhD, Yei Hwan Jung, Xian Huang, PhD, Fiorenzo G. Omenetto, PhD, John A. Rogers, PhD, and Michael R. Bruchas, PhD

Department of Materials Engineering, University of Illinois
Urbana-Champaign, Illinois
Departments of Anesthesiology and Neurobiology
Washington University in St. Louis
St. Louis, Missouri

© 2013 Bruchas

NOTES

Introduction

In neuroscience generally, and in optogenetics in particular, an ability to insert light sources, detectors, sensors, and other components into precise locations of the deep brain could yield versatile and important capabilities. Here, we introduce an injectable class of cellular-scale optoelectronics that offers such features, with examples of unmatched operational modes in optogenetics. These include completely wireless and programmed behavioral control over freely moving animals.

Electronic systems that integrate with the body provide powerful diagnostic and therapeutic capabilities for basic research and clinical medicine. Recent research establishes materials and mechanical constructs for electronic circuits, light emitting diodes (LEDs), sensors, and other components that can wrap the soft, external surfaces of the brain, skin, and heart for diverse function in analytical measurement, stimulation, and intervention (Sekitani et al., 2009; Qing et al., 2010; Tian et al., 2010; Viventi et al., 2010; Kim et al., 2010, 2011). A significant constraint in operating these devices, however, follows from their surface-mounted configurations and inability to provide direct interaction into the volumetric depths of tissues. Passive penetrating electrodes or optical fibers with interconnections to externally located electronic control/acquisition systems or light sources can be valuable in many contexts—particularly in neuroscience, engineering, and surgery (Anikeeva et al., 2012; Mattis et al., 2012; Stark et al., 2012). Direct biological integration is limited by challenges from tissue lesions during insertion, persistent irritation, and engineering difficulties in thermal management, encapsulation, scalable interconnection, power delivery, and external control. Many of these issues constrain attempts to insert conventional bulk LEDs into brain tissue (Kim et al., 2012b) and to use semiconductor nanowire devices as cellular probes or active, *in vitro* tissue scaffolds (Tian et al., 2010, 2012).

In optogenetics, engineering limitations of conventional, tethered fiber optic devices restrict opportunities for *in vivo* use and widespread biological application. As a solution, we developed mechanically compliant, ultrathin multifunctional optoelectronic systems that mount on releasable injection needles for insertion into the depth of soft tissue. These wireless devices incorporate cellular-scale components ranging from independently addressable, multicolored microscale inorganic light-emitting diodes (μ-ILEDs) to colocated, precision optical, thermal, and electrophysiological sensors and actuators.

Design and Function of Wireless Optoelectronics

Figure 1*A* presents a scanning electron micrograph (SEM) of an isolated gallium nitride (GaN) μ-ILED, as a constituent component of these systems, and an epifluorescent image of a device among cultured HEK293 cells to illustrate the similar sizes. Each such "cellular-scale" μ-ILED (6.45 μm thick, 50 × 50 μm^2) uses high-quality epitaxial material grown on sapphire, processed to establish contacts (15 × 15 μm^2 square pads in the corners, and an L-shaped current-spreading layer for the p-contact) and then released, to allow transfer printing onto narrow, thin plastic strips. The μ-ILEDs are more than 1,000 times smaller than conventional LEDs (typically 100 μm thick, with lateral dimensions of 1 mm^2) and fiber optic probes (Kim et al., 2012b). The small sizes of μ-ILEDs allow for spatially precise, cellular-scale delivery of photons, highly effective thermal management, limited power requirements, reduced tissue damage, and minimized inflammation for prolonged use *in vivo*.

Combining μ-ILEDs with electronic sensors and actuators yields multifunctional integrated systems that can be configured in single or multilayer formats. Figures 1*B* and *C* illustrate the latter option. In this format, the sensors/actuators include the following: a microelectrode for electrophysiological recording or electrical stimulation (Layer #1; a 20 × 20 μm^2 exposure defines the active area); a microscale inorganic photodetector (μ-IPD) based on an ultrathin silicon photodiode (Layer #2; 1.25 μm thick, 200 × 200 μm^2); a collection of 4 μ-ILEDs connected in parallel (Layer #3); and a precision temperature microsensor or microheater (Kim et al., 2013). Each layer is processed on separate substrates shaped to match a releasable, photolithographically defined epoxy microneedle. A thin layer (~500 nm) of epoxy joins each layer in a precisely aligned, stacked configuration. The microneedle bonds to the bottom layer with a thin, bioresorbable silk fibroin, enabling removal of the microneedle after implantation (Fig. 1*D*). The temperature sensors determine the degree of local heating, with a precision approaching ~1 mK, and can be used as microheaters. The μ-IPD can measure the intensity of light from the μ-ILEDs while implanted deep in brain tissue and/or enable basic spectroscopic evaluations of absorption, fluorescence, diffuse scattering, etc. (Kim et al., 2013).

© 2013 Bruchas

NOTES

Implantation and Device Function

Injection of such flexible devices into the brain follows the steps shown in Figure 1*D*. The injected multifunctional optoelectronic systems have a total thickness of ~20 μm. This exceptionally thin geometry, low bending rigidity, and high degree of mechanical flexibility (Figs. 1*E*, *F*) allow for minimally invasive operation. Wired control schemes use standard transistor–transistor logic (TTL) and are therefore compatible with any electrical commutators. Details on wired powering strategies and optogenetic functionality in rodent behavioral assays are presented in Kim et al., 2013.

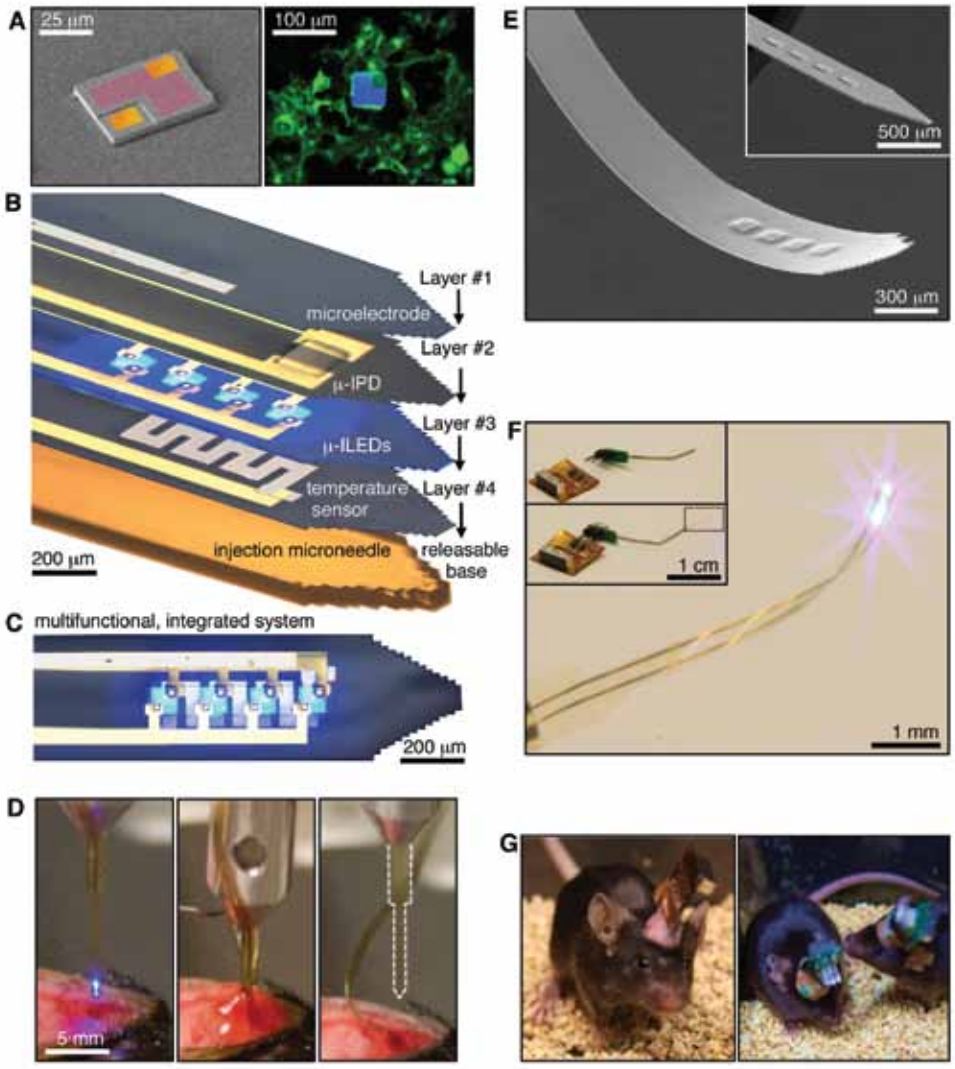

Figure 1. Injectable, cellular-scale semiconductor devices, with multifunctional operation in stimulation, sensing, and actuation. ***A,*** Left, colorized SEM of a GaN μ-ILED (~6.45 μm thick, and 50 × 50 μm^2; contacts: gold; spreading layer: red). Right, fluorescent image of a μ-ILED (blue) with cultured HEK293 cells that express an eYFP-tagged transmembrane protein (green). ***B,*** A multifunctional, implantable optoelectronic device, in a tilted exploded-view layout illustrating various components. The system includes layers for electrophysiological measurement (layer #1; Pt contact pad, microelectrode), optical measurement (layer #2; silicon μ-IPD), optical stimulation (layer #3; μ-ILED array), and temperature sensing (layer #4; serpentine Pt resistor), all bonded to a releasable structural support for injection (microneedle). ***C,*** Top view of the integrated device shown in *B*. ***D,*** Process of injection and release of the microneedle. After insertion, artificial cerebrospinal fluid (center) dissolves the external silk-based adhesive. The microneedle is removed (right), leaving only the active device components in the brain. ***E,*** SEM of an injectable array of μ-ILEDs. The total thickness is 8.5 μm. Inset shows rigid device before coating with a passivation layer. ***F,*** Integrated system wirelessly powered with RF scavenging. Insets show a connectorized device unplugged (top) and plugged into (bottom) the wireless power system. ***G,*** Healthy, freely moving mice with lightweight, flexible (left) and rigid (right) wireless systems powering GaN μ-LED arrays in the VTA. Scale bars: ***A,*** Left, 25 μm; right, 100 μm; ***B,*** 200 μm; ***C,*** 200 μm; ***D,*** 5 mm; ***E,*** 300 μm; inset, 500 μm; ***F,*** 1 mm; insets, 1 cm.

© 2013 Bruchas

NOTES

Figure 1*F* shows the implementation of a wireless power module based on radiofrequency (RF) scavenging. A custom flexible polyimide film-based lightweight (~0.7 g) power scavenger or a rigid printed circuit board–based scavenger (~2.0 g; Fig. 1G) can be acutely and temporarily mounted on freely moving animals without constraining their natural animal behavior (Fig. 1G). The entire system consists of a wireless power transmitter and RF signal generator; an RF source (910 MHz; power output between 0.02 and 0.1 mW); a power supply; an RF power amplifier (gain of 49 dB at 910 MHz; power output between 1.6 and 7.9 W); and a panel antenna (gain of 13 dBi). The low-frequency signal generator provides user-controlled amplitude modulation for programmed operation. The RF power that reaches the animals, under normal operating conditions at a distance of ~1 m, is between 0.15 and 0.77 mW/cm^2, which is substantially smaller than the maximum permissible exposure (MPE) limits (3.03 mW/cm^2) for humans (FCC). Wireless control allows access to complex and ethologically relevant models in diverse environmental settings, including social interactions, home-cage behaviors, wheel running, complex maze navigation tasks, and many other behavioral outputs (Fig. 1G).

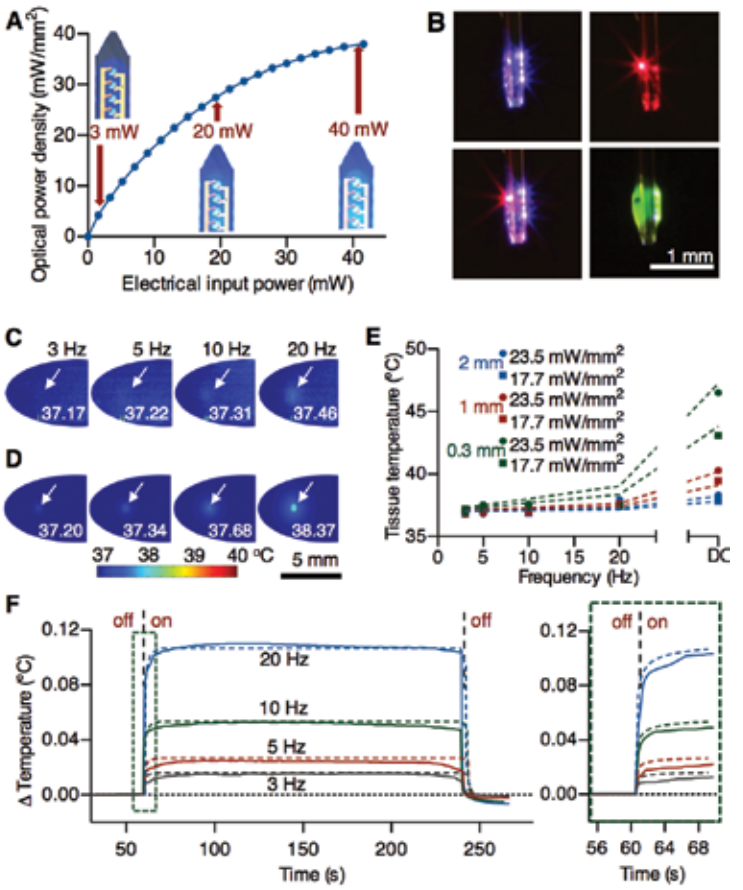

Figure 2. Optical, thermal, and electrophysiological studies with corresponding theoretical analyses. ***A,*** Total optical power density as a function of electrical input power applied to an array of four GaN μ-ILEDs; optical images show operation at 3, 20, and 40 mW. ***B,*** A single device has one 675 nm GaAs μ-ILED and four 450 nm GaN μ-ILEDs that can be activated either independently (top left and top right) or concurrently (bottom left). The same device is coated in a fluorescein sodium salt phosphor for 530 nm light (bottom right). ***C,*** Measured and ***D,*** calculated temperatures in explanted brain tissue near implanted μ-ILEDs at a depth of 0.3 mm and operated at 17.7 mW/mm^2 of light output power. ***E,*** Temperatures in a system similar to that of *C* and *D,* as a function of duty cycle in the operation of the μ-ILEDs and at three different implantation depths (0.3, 1.0, and 2.0 mm) and two different light output powers (17.7 and 23.5 mW/mm^2). ***F,*** Change in brain temperature as a function of time, measured using an integrated temperature sensor colocated with an array of four μ-ILEDs in a lightly anesthetized mouse. Results were evaluated at peak input electrical power of 8.65 mW, in 3, 5, 10, and 20 Hz pulses (10 ms duration). The vertical dashed lines indicate onset (at 60 s) and offset (at 240 s) of the μ-ILEDs. Colored dashed lines correspond to theoretical models for the temperature. The right frame shows the time dynamics as the device is powered. Scale bars: ***B,*** 1 mm; ***C, D,*** 5 mm.

The electrical, optical, and thermal characteristics of the devices when operated in biological environments are important for optogenetics and other biomedical applications. Figure 2A shows the total optical power density of the 4 μ-ILEDs in this device as a function of electrical input power (Kim et al., 2013). This performance is comparable with similarly designed, state-of-the-art conventional GaN LEDs (Kim et al., 2013). Many optogenetic constructs can be activated with ~1 mW/mm^2, at wavelengths near 450 nm (Mattis et al., 2012). These conditions are well matched to the output of the GaN μ-ILEDs. An input power of ~1.0–1.5 mW (Fig. 2A) is sufficient for both activation of the channelrhodopsin-2 (ChR2(H134)) ion channel and precise control of intracellular signaling (cAMP and ERK 1/2) via an optically sensitive G-protein coupled receptor (Optoβ2) (Figs. 3C, *D*, 5) (Airan et al., 2009). Wirelessly, at a distance of 1 m, the RF scavenger outputs 4.08 mW of electrical power, resulting in a 7 mW/mm^2 optical power density.

© 2013 Bruchas

NOTES

Other wavelengths are possible using different types of μ-ILEDs, either in multicolored or uniform arrays. Figure 2*B* shows an example of the latter, with blue and red gallium arsenide (GaA) μ-ILEDs, and the former, with green devices.

Figures 2C and *D* show μ-ILED–induced changes in temperature determined by infrared imaging and analytical calculation, respectively. The μ-ILEDs were implanted 0.3 mm into an explanted piece of brain tissue held at 37°C. The time-averaged temperatures measured at light-pulse (10 ms) frequencies of 3, 5, 10, and 20 Hz with peak light output of 17.7 mW/mm2 are 37.17°, 37.22°, 37.31°, and 37.46°C, respectively. These results are similar to calculated time-averaged temperatures of 37.20°, 37.34°, 37.68°, and 38.37°C, respectively. The input power used in these tests is 10 times greater than what is necessary to activate many optogenetic constructs (Mattis et al., 2012). The cellular-scale dimensions of the μ-ILEDs enable high rates of thermal spreading, and the brain tissue operates as an efficient heat sink. The latter property is apparent in studies of the dependence of operating temperature on tissue thickness, operating power, and frequency (Fig. 2E). (More details appear in Kim et al., 2013.) Figure 2F shows changes in temperature measured *in vivo* using an integrated temperature sensor compared with calculated results.

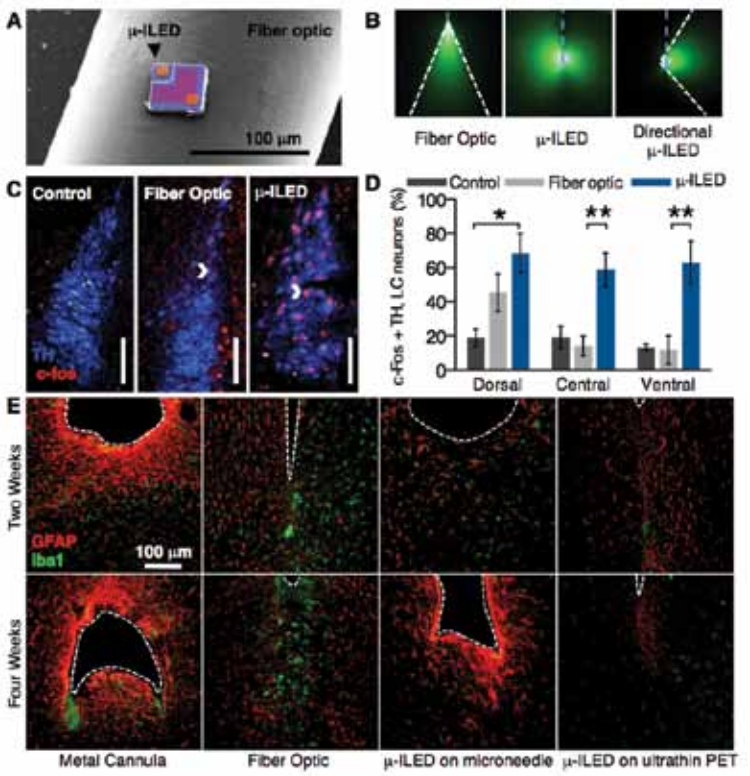

Figure 3. μ-ILED devices improve spatial targeting and reduce gliosis. ***A,*** Colorized SEM (left) of a μ-ILED mounted on a standard 200 μm fiber optic implant. ***B,*** Left, a dorsal-ventral–oriented light cone (outlined in white) from a 200 μm bare fiber implant (blue dashes) emitting 465 nm light in 30 μM fluorescein water. Center, near-omnidirectional light escape from a μ-ILED device (blue dashes) with four 450 nm μ-ILEDs. Right, lateral light escape (outlined in white) from a modified μ-ILED device (blue dashes) to allow unique spatial targeting, including flanking positions along the dorsal-ventral axis of brain loci. ***C,*** Confocal fluorescence images of 30 μm brainstem slices containing the LC show staining for tyrosine hydroxylase (TH, blue) and c-Fos (red) in control (left), fiber optic implanted (center), and μ-ILED device–implanted (right) animals following 1 h, 3 Hz photostimulation (15 ms pulses; 5 mW output power). ***D,*** Fiber optic and μ-ILED treatments specifically increase coimmunoreactivity. Ventral portions of the LC the μ-ILED devices express a higher proportion of tyrosine hydroxylase (TH) and c-Fos coimmunoreactive neurons than fiber optic or control groups (n = 3 slices per brain from 3 brains for each group; two-way ANOVA with Bonferroni's test; all error bars represent means ± SEM; $^{*}p < 0.05$, $^{**}p < 0.01$). ***E,*** Confocal fluorescence images of 30 μm striatal slices show staining for astrocytes (GFAP, red) and activated microglia (Iba1, green) at the ventral tip of each implanted device (dashed outline). Gliosis is smallest with the μ-ILED device at both 2-week and 4-week time points. Scale bars: ***A, C, E,*** 100 μm. PET, positron emission tomography.

Collectively, these results indicate that changes in temperature associated with the operation of μ-ILEDs can be less than 0.10°C for pulse frequencies less than 20 Hz, typical of many neuronal firing rates and lower than those that occur in human deep-brain stimulation (DBS) regulation, ~2°C (Elwassif et al., 2006). In wireless operation, no appreciable change in temperature is associated with operation at the head-stage antenna or skull. To demonstrate functionality of the silicon μ-IPD, Figure 2G shows photocurrents generated by different intensities of light from μ-ILEDs at different pulse frequencies. Finally, the Pt microelectrode has a 400 μm^2 exposure site with ~1.0 MΩ impedance at 1 kHz, capable of measuring extracellular potentials on the μV scale for distinguishing individual action potentials (Figs. 2*H, I*).

In Vivo Operation: Wireless Optical Control of Behavior

For use in optogenetics, such devices eliminate the need for lasers, bulk LEDs, fiber coupling systems, tethers, and

© 2013 Bruchas

NOTES

optomechanical hardware used in conventional approaches. Absorbing/reflecting structures around the emissive areas of the μ-ILEDs enable precise delivery of light to cellular subregions. Figures 3*A* and *B* compare relative size and the different patterns of light emission from μ-ILEDs with fiber optic probes. Fiber optics typically approach brain structures dorsally. This approach preferentially illuminates cells in the dorsal portion of the targeted region, with greater light intensity near the point of light escape (Fig. 3*B*, left) (Aravanis et al., 2007). Targeting ventral cell bodies or terminals requires lesion of dorsal regions or the use of substantially greater, potentially phototoxic (Yizhar et al., 2011) amounts of light to the site of interest. Neither option protects the intact architecture of a complete brain locus. Though recent advances have spatially restricted light from implanted fiber optics (Tye et al., 2011; Zorzos et al., 2012), these approaches require invasive metal cannulae (Fig. 3*E*) or rely on sophisticated and sensitive engineering that may limit their use in awake, behaving animals. The architecture of the μ-ILEDs enables light delivery medial or lateral to the intended target brain region. Native light escape from μ-ILEDs is nearly omnidirectional (Fig. 3*B*, center) but can be restricted to a wide range of angles with absorbing or reflective structures on the device (Fig. 3*B*, right).

We acutely implanted both μ-ILEDs and fiber optics into animals expressing ChR2(H134)-eYFP in the locus ceruleus (LC). One hour of output-matched photostimulation induced c-fos expression, a biochemical marker of neuronal activation, in both groups of ChR2(H134)-eYFP–expressing mice that was not seen in green fluorescent protein (GFP)–expressing controls (Figs. 3*C, D*). The spatial distribution of c-Fos expression, however, differed markedly between the fiber optic and μ-ILED groups. μ-ILED devices produced significantly greater activation in the ventral LC (Fig. 3*D*).

The physical sizes and mechanical properties of the μ-ILED systems reduce lesioning, neuronal loss, gliosis, and immunoreactivity. Glial responses are biphasic, with an early phase featuring widespread activation of astrocytes and microglia, and a late, prolonged phase hallmarked by restriction

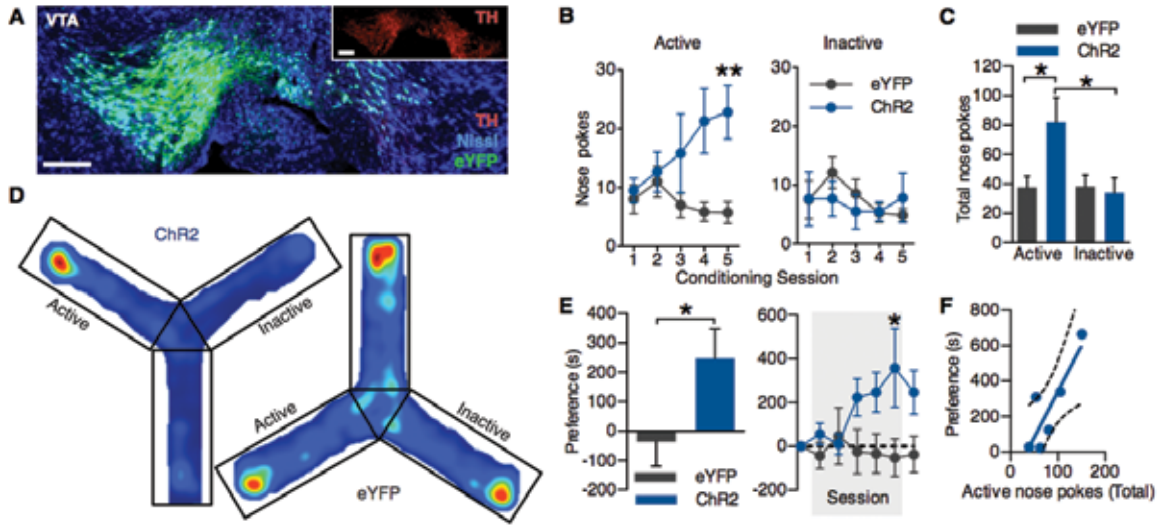

Figure 4. Wirelessly powered μ-ILED devices operantly drive-conditioned place preference. ***A,*** Cell type–specific expression of ChR2(H134)-eYFP (green) in dopaminergic, TH (red)–containing neurons of the VTA. For clarity, inset shows TH channel alone. All scale bars = 100 μm. ***B,*** Operant learning curve on the active (left) and inactive (right) nose poke devices over 5 days of 1 h trials in the Y-maze. Active pokes drive 1 s of 20 Hz light (5 ms pulses) from the μ-ILED device on a fixed-ratio-1 schedule (n = 6–8 mice/group; two-way ANOVA with Bonferroni's test; $^{**}p < 0.01$). ***C,*** Mean number of nose pokes ± SEM across all 5 conditioning sessions. ($^{*}p < 0.05$; one-way ANOVA with Bonferroni's test). ***D,*** Heat maps of activity during the posttest; hotter colors represent longer duration in a location in that part of the apparatus. ***E,*** Left, place preference scores calculated as posttest minus pretest in the active nose poke–paired context. Five days of self-stimulation significantly conditioned a place preference that developed over the course of the training sessions and remained during the posttest (right; $^{*}p < 0.05$ t test compared with controls; $^{*}p < 0.05$ two-way ANOVA with Bonferroni's test). All error bars represent means ± SEM. ***F,*** Scatter plot demonstrating positive correlation ($r = 0.8620$; $p = 0.0272$) between posttest preference and total number of active nose pokes during training in the ChR2(H134)-eYFP group.

© 2013 Bruchas

NOTES

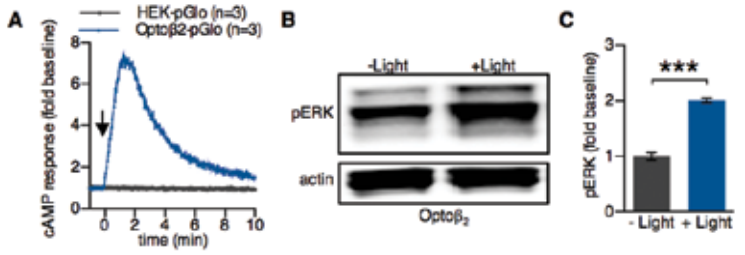

Figure 5. μ-ILED–induced activation of cAMP and ERK phosphorylation in Optoβ2-expressing cells. ***A***, Optoβ2 cells coexpressing pGlo show a rapid and transient increase in cAMP following light (450 nm, 5 s, 0.5 W/cm^2 pulse) stimulation ($n = 3$). HEK293 cells expressing pGlo show no response to the same light stimulation ($n = 3$). Data are expressed as mean ± SEM. ***B***, Representative pERK and actin Western blots for Optoβ2 and HEK293 cells following light (450 nm, 1 min, 0.5 W/cm^2 pulse) stimulation ($n = 3$). ***C***, Quantitation of pERK normalized to actin in light-stimulated Optoβ2 and HEK293 cells (*$p < 0.05$; unpaired, two-tailed *t* test).

of the gliosis to the area closest to the implanted substrate (Szarowski et al., 2003). The μ-ILED devices produced substantially less glial activation and caused smaller lesions as compared with metal cannulae and fiber optics, at both early (2 weeks) and late (4 weeks) phases (Fig. 3*E*). Furthermore, the brain tolerates the thin, flexible devices better than rigid structures (Fig. 3*E*), consistent with reports on passive electrode devices (Kozai and Kipke, 2009). Finally, we examined the chronic functionality of the devices and demonstrated that they are well tolerated in freely moving animals with encapsulated sensors and μ-ILEDs, maintaining function over 3–6 months.

We next implemented a fully wireless system for dissecting complex neurobiology and behavior. Phasic neuronal firing of ventral tegmental area–dopaminergic (VTA-DA) neurons encodes salient stimuli and is sufficient for behavioral conditioning (Tsai et al., 2009; Adamantidis et al., 2011; Coque et al., 2011; Kim et al., 2012a). We selectively targeted ChR2(H134)-eYFP to VTA-DA neurons (Fig. 4*A*) and tested whether mice would engage in wireless, optical self-stimulation (5 ms pulses every nose poke) of their dopamine reward pathway. To increase the contextual salience of the stimulation and demonstrate wireless function of the μ-ILED devices, the mice were free to explore a complex environment. In the absence of physical reward, the same stimulation of VTA-DA neurons that drives a traditionally conditioned place preference (Tsai et al., 2009; Adamantidis et al., 2011) is actively sought with a cued nose poke when paired within a discrete environmental context. ChR2(H134)-eYFP mice learned to self-stimulate their dopamine neurons (Figs. 4*B*, *C*) and, furthermore, developed a robust place preference (Figs. 4*D*, *E*) for the environmental context containing the active nose poke for VTA-DA stimulation. ChR2(H134)-eYFP animals showed a strong correlation ($r = 0.8620$; $p = 0.0272$) between the number of active nose pokes and the magnitude of conditioned place preference that was absent in eYFP controls (Fig. 4*F*).

In addition, we examined the effects of wireless tonic stimulation of VTA-DA neurons on anxiety-like behavior. Five hertz tonic stimulation reduced anxiety-like behavior, whereas phasic activation of VTA-DA neurons did not have an effect on anxiety-like behavior. These findings are consistent with the anxiolytic actions of nicotine on VTA-DA neurons as well as the behavioral phenotypes seen in the *Clock*Δ19 mice that have increased tonic firing of VTA-DA neurons (Coque et al., 2011; McGranahan et al., 2011). They further establish the utility of wireless optogenetic control in multiple environmental contexts.

Conclusion

These experiments demonstrate that these wireless devices can be readily used in optogenetic experiments. Future possible uses are in closed-loop operation, where actuators (heat, light, electrical, etc.) operate in tandem with sensors (temperature, light, potential, etc.) for altering light stimulation in response to physiological parameters such as single-unit activity, pH, blood oxygen or glucose levels, and neurochemical changes associated with neurotransmitter release. Many of the attributes that make these devices useful in optogenetics suggest they also have strong potential for broader use in biology and medicine. The demonstrated compatibility of silicon technology in these injectable, cellular-scale platforms foreshadows sophisticated capabilities in electronic processing and biological interfaces. Biocompatible deep-tissue injection of semiconductor devices and integrated systems such as those reported here will accelerate progress in both basic neuroscience and translational technologies.

© 2013 Bruchas

NOTES

Acknowledgments

This work is supported by the National Institutes of Health Common Fund, the National Institute of Neurological Disorders and Stroke Grant R01NS081707 (M.R.B., J.A.R.), the National Institute on Drug Abuse Grant R00DA025182 (M.R.B.), the McDonnell Center for Systems Neuroscience (M.R.B.), National Security Science and Engineering Faculty Fellowship of Energy (J.A.R.), U.S. Department of Energy, Division of Materials Sciences under Award No. DE-FG02-07ER46471 (J.A.R.), the Materials Research Laboratory and Center for Microanalysis of Materials (DE-FG02-07ER46453) (J.A.R.), and Washington University in St. Louis Division of Biology and Biomedical Sciences (WUSTL DBBS) (J.G.M.). We thank Hu Tao (Tufts University) and Sukwon Hwang (University of Illinois, Urbana-Champaign) for their help in preparing the silk solution. We thank the Bruchas laboratory and Robert W. Gereau, IV (WUSTL) and Garret D. Stuber (University of North Carolina) for helpful discussion. We thank Karl Deisseroth (Stanford University) for the channelrhodopsin-2 (H134) and OPTO-β2 constructs, G. Stuber for the TH-IRES-Cre mice, the WUSTL Bakewell Neuroimaging Laboratory Core, and the WUSTL Hope Center Viral Vector Core. This chapter is a modified version of a previously published article: Kim TI, et al. *Science*. 2013;340:211–216.

References

Adamantidis AR, Tsai H-C, Boutrel B, Zhang F, Stuber GD, Budygin EA, Touriño C, Bonci A, Deisseroth K, De Lecea L (2011) Optogenetic interrogation of dopaminergic modulation of the multiple phases of reward-seeking behavior. J Neurosci 31:10829–10835.

Airan RD, Thompson KR, Fenno LE, Bernstein H, Deisseroth K (2009) Temporally precise *in vivo* control of intracellular signalling. Nature 458:1025–1029.

Anikeeva P, Andalman AS, Witten I, Warden M, Goshen I, Grosenick L, Gunaydin LA, Frank LM, Deisseroth K (2012) Optetrode: a multichannel readout for optogenetic control in freely moving mice. Nat Neurosci 15:163–170.

Aravanis AM, Wang L-P, Zhang F, Meltzer LA, Mogri MZ, Schneider MB, Deisseroth K (2007) An optical neural interface: *in vivo* control of rodent motor cortex with integrated fiberoptic and optogenetic technology. J Neural Eng 4:S143–S156.

Coque L, Mukherjee S, Cao J-L, Spencer S, Marvin M, Falcon E, Sidor MM, Birnbaum SG, Graham A, Neve RL, Gordon E, Ozburn AR, Goldberg MS, Han M-H, Cooper DC, McClung CA (2011) Specific role of VTA dopamine neuronal firing rates and morphology in the reversal of anxiety-related, but not depression-related behavior in the *Clock*Δ19 mouse model of mania. Neuropsychopharmacology 36:1478–1488.

Elwassif MM, Kong Q, Vazquez M, Bikson M (2006) Bio-heat transfer model of deep brain stimulation-induced temperature changes. J Neural Eng 3:306–315.

Kim D-H, Viventi J, Amsden JJ, Xiao J, Vigeland L, Kim Y-S, Blanco JA, Panilaitis B, Frechette ES, Contreras D, Kaplan DL, Omenetto FG, Huang Y, Hwang K-C, Zakin MR, Litt B, Rogers JA (2010) Dissolvable films of silk fibroin for ultrathin conformal bio-integrated electronics. Nat Mater 9:511–517.

Kim D-H, Lu N, Ma R, Kim YS, Kim RH, Wang S, Wu J, Won SM, Tao H, Islam A, Yu KJ, Kim TI, Chowdhury R, Ying M, Xu L, Li M, Chung HJ, Keum H, McCormick M, Liu P, et al. (2011) Epidermal electronics. Science 333:838–843.

Kim KM, Baratta MV, Yang A, Lee D, Boyden ES, Fiorillo CD (2012a) Optogenetic mimicry of the transient activation of dopamine neurons by natural reward is sufficient for operant reinforcement. PLoS One 7:e33612.

Kim TI, Jung YH, Song J, Kim D, Li Y, Kim H, Song I-S, Wierer JJ, Pao HA, Huang Y, Rogers JA (2012b) High-efficiency, microscale GaN light-emitting diodes and their thermal properties on unusual substrates. Small 8:1643–1649.

Kim TI, McCall JG, Jung YH, Huang X, Siuda ER, Li Y, Song J, Song YM, Pao HA, Kim RH, Lu C, Lee SD, Song IS, Shin G, Al-Hasani R, Kim S, Tan MP, Huang Y, Omenetto FG, Rogers JA, et al. (2013) Injectable, cellular-scale optoelectronics with applications for wireless optogenetics. Science 340:211–216.

Kozai TDY, Kipke DR (2009) Insertion shuttle with carboxyl terminated self-assembled monolayer coatings for implanting flexible polymer neural probes in the brain. J Neurosci Methods 184:199–205.

© 2013 Bruchas

NOTES

Mattis J, Tye KM, Ferenczi EA, Ramakrishnan C, O'Shea DJ, Prakash R, Gunaydin LA, Hyun M, Fenno LE, Gradinaru V, Yizhar O, Deisseroth K (2012) Principles for applying optogenetic tools derived from direct comparative analysis of microbial opsins. Nat Methods 9:159–172.

McGranahan TM, Patzlaff NE, Grady SR, Heinemann SF, Booker TK (2011) α4β2 nicotinic acetylcholine receptors on dopaminergic neurons mediate nicotine reward and anxiety relief. J Neurosci 31:10891–10902.

Qing Q, Pal SK, Tian B, Duan X, Timko BP, Cohen-Karni T, Murthy VN, Lieber CM (2010) Nanowire transistor arrays for mapping neural circuits in acute brain slices. Proc Natl Acad Sci USA 107:1882–1887.

Sekitani T, Yokota T, Zschieschang U, Klauk H, Bauer S, Takeuchi K, Takamiya M, Sakurai T, Someya T (2009) Organic nonvolatile memory transistors for flexible sensor arrays. Science 326:1516–1519.

Stark E, Koos T, Buzsáki G (2012) Diode probes for spatiotemporal optical control of multiple neurons in freely moving animals. J Neurophysiol 108:349–363.

Szarowski DH, Andersen MD, Retterer S, Spence AJ, Isaacson M, Craighead HG, Turner JN, Shain W (2003) Brain responses to micro-machined silicon devices. Brain Res 983:23–35.

Tian B, Cohen-Karni T, Qing Q, Duan X, Xie P, Lieber CM (2010) Three-dimensional, flexible nanoscale field-effect transistors as localized bioprobes. Science 329:830–834.

Tian B, Liu J, Dvir T, Jin L, Tsui JH, Qing Q, Suo Z, Langer R, Kohane DS, Lieber CM (2012) Macroporous nanowire nanoelectronic scaffolds for synthetic tissues. Nat Mater 11:986–994.

Tsai H-C, Zhang F, Adamantidis A, Stuber GD, Bonci A, De Lecea L, Deisseroth K (2009) Phasic firing in dopaminergic neurons is sufficient for behavioral conditioning. Science 324:1080–1084.

Tye KM, Prakash R, Kim S-Y, Fenno LE, Grosenick L, Zarabi H, Thompson KR, Gradinaru V, Ramakrishnan C, Deisseroth K (2011) Amygdala circuitry mediating reversible and bidirectional control of anxiety. Nature 471:358–362.

Viventi J, Kim D-H, Moss JD, Kim Y-S, Blanco JA, Annetta N, Hicks A, Xiao J, Huang Y, Callans DJ, Rogers JA, Litt B (2010) A conformal, bio-interfaced class of silicon electronics for mapping cardiac electrophysiology. Sci Transl Med 2:24ra22.

Yizhar O, Fenno LE, Davidson TJ, Mogri M, Deisseroth K (2011) Optogenetics in neural systems. Neuron 71:9–34.

Zorzos AN, Scholvin J, Boyden ES, Fonstad CG (2012) Three-dimensional multiwaveguide probe array for light delivery to distributed brain circuits. Opt Lett 37:4841–4843.

© 2013 Bruchas

Optogenetic Tools for Mesoscopic-Level Imaging Approaches: Bridging Cellular-Level and Systems Physiology

Thomas Knöpfel, MD, PhD

Division of Brain Sciences
Imperial College London
London, United Kingdom

© 2013 Knöpfel

NOTES

The great topmost sheet of the mass, that where hardly a light had twinkled or moved, becomes now a sparkling field of rhythmic flashing points with trains of traveling sparks hurrying hither and thither.

—Charles S. Sherrington, *Man on his Nature* (1940)

Introduction

Since Charles S. Sherrington's poetic expression of these rather philosophical thoughts, a popular metaphor for neuronal activities has been "sparks of light." However, the advance from imagination to imaging would require dyes that could transform neuronal activity into optical signals (e.g., modulation of fluorescence intensities). The first optical activity–indicator dyes were voltage-sensitive ones, which were then followed and complemented by calcium indicators. Under many experimental conditions, calcium imaging provides a better signal-to-noise ratio (SNR) than voltage indicators. And it is for this reason that the former have become the more widely adopted tool for experimental monitoring of neuronal activities, realizing the vision of Sherrington.

In combination with two-photon (2P) microscopy, calcium imaging enables the tracking of action-potential events from hundreds (<1,000) of neurons simultaneously in living rodents. Voltage imaging is preferred in experimental paradigms where not the single cell, but large populations of cells (>1,000) distributed over larger (typically cortical) areas, are the focus of interest. Voltage imaging at this mesoscopic scale (fields of view at the millimeter scale) has clear advantages over calcium imaging: higher temporal resolution and the ability to report subthreshold synaptic potentials. Although classical mesoscopic voltage-sensitive dye imaging (VSDI) contributed many important insights on cortical circuit dynamics, VSDI gives information on neuronal activities that are averaged over heterogeneous, large cell populations. Therefore, it cannot reflect on the role of specific cell classes and is limited to activities synchronized over large numbers of cells. A solution to overcome this limitation emerged with the availability of bright fluorescent proteins (FPs), which have been used to engineer genetically encoded calcium indicators (GECIs) and genetically encoded voltage indicators (GEVIs) (Alford et al., 2013; Mutoh and Knöpfel, 2013).

Optical imaging using GECIs and GEVIs takes aim at the two general obstacles that brain sciences must overcome. The first arises from the fact that neuronal circuits generate and process signals through microscopic and numerous parallel channels at the millisecond timescale. Optical methods provide a measurement technology in order to accurately detect these signals with the required spatial and temporal resolution. The second obstacle is, as mentioned above, the requirement to account for neuronal diversity. The brain features a complex composition of varied cell types, each of which has different intrinsic properties and modes of intercellular interaction. Because of this diversity, the function of neuronal circuits cannot be deduced from the functional properties of a single representative cell type. By genetically targeting defined populations of neurons, however, it becomes feasible to identify, monitor, and control specific cell classes in their functional context.

GECIs and GEVIs can be categorized as components of the optogenetic toolbox (Dugué et al., 2012). Some authors restrict the term "optogenetics" to approaches designed to manipulate neuronal activities with light (in particular, using opsins). However, we prefer the more general definition of optogenetics as a methodological platform based on optics and genetics to investigate the function of specific cells in heterologous tissues by monitoring and manipulating their physiological activities. Thus, just as traditional electrophysiology uses electrical wires and electrodes for recording and stimulating electrically active cells, optogenetic approaches use light and genetic targeting to elucidate (neuro) physiological mechanisms.

Bridging Cellular-Level and Systems Physiology

For any slightly complex behavior, the number of neurons involved in its generation is very large. Based on the conjecture that behavior emerges only from the activities of very large numbers of neurons, a (full) record of neuronal activity across the whole intact brain embedded in a behaving animal would, in principle, be required to (fully) decipher the link between neuronal action potentials and behavior.

Unfortunately, a full record of neuronal activity across the whole intact brain in a behaving mammal is far beyond our current technical reach. Although enabling technologies toward that ambitious aim are on the agenda of the BRAIN initiative (Insel et al., 2013), the current practical advance requires us to compromise with respect to at least one of several areas: the number of neurons, the size of the observation field or volume, or the temporal resolution when recording neuronal activities. Another strategy is to employ recording techniques that allow one to monitor the activities of very large number of cells while favoring

© 2013 Knöpfel

NOTES

population signals at the sacrifice of single-cell resolution. Examples of such a compromise include approaches such as local field potential recordings, electroencephalography (EEG), electrocorticography (ECoG), and magnetoencephalography (MEG).

The basic argument that circuit analysis can be insightful without resolving individual cells builds on the well-established fact that many brain systems use temporal correlations in the action potential output of individual neurons. These correlated action potential activities are associated with robust synchrony of membrane voltage fluctuation, reflecting a common time structure of the received synaptic input as well as dynamic properties of the imbedding circuits. But again, the caveat of traditional large-scale population recordings is that they are blind to cellular diversity. That is, they generally even fail to tell which cell classes are involved in the observed population activities. These approaches therefore cannot provide a solid link between cellular and circuit mechanisms. Genetically encoded (optogenetic) indicators overcome this limitation by enabling population imaging of defined cell classes (Knöpfel et al., 2006; Knöpfel, 2012).

Genetically encoded calcium indicators

The basic design idea of all current GECIs follows that of organic fluorescent calcium indicators. In the latter, a calcium-binding molecule is combined with a bright fluorescent dye in a manner that results in a change in fluorescence output upon binding of calcium. The first GECIs used the calcium-binding calmodulin-M13 complex and FPs as building blocks. Troponin C was introduced a few years later as an alternative calcium-binding protein suitable for the generation of GECIs. The calcium binding–induced conformational state transition is coupled to a conformation-sensitive FP-based reporter component. This conformation sensitivity can be achieved either by modulating the efficiency of Förster resonance energy transfer (FRET, also known as fluorescence resonance energy transfer) between a pair of FPs, or by destabilizing the FP chromophore via circular permutation (cp) of its protective barrel structure. This reporting mechanism led to the vast variety of useful monochromatic (single FP) GECIs. In the most widely used GCaMP-type configuration, elevated calcium concentrations increase the quantum yield of fluorescence, observed as a large increase in fluorescence.

Parallel efforts by several groups have given rise to a set of well-performing GECIs with distinctive physiochemical features. The most critical characteristics of different GECIs are the photophysical properties of the FPs used and the effective calcium-binding kinetics. A high affinity for calcium (low K_d value) is favorable for smaller calcium signals (e.g., those associated with single narrow action potentials); however, a low K_d value also results in indicator saturation during high-frequency bursts of action potentials and causes higher baseline fluorescence. Far-red or infrared-shifted probes would be preferable in view of the fact that tissue autofluorescence peaks at greenish wavelengths, but the photophysical properties (i.e., fluorescence quantum yield and stability) are usually inferior in red-shifted FPs as compared with their greenish variants. Moreover, 2P excitation has been much less rigorously established for probes with fluorescence emission in the far-red and infrared portion of the spectrum. Several groups have tried to rigorously and directly compare GECIs under specific experimental conditions. Although their work is incomplete, it has shown that under different experimental requirements, different GECI variants are preferable. In practice, the choice of an appropriate GECI also depends on the available instrumentation and access to animals or viruses with specific indicator genes. The most widely used GECIs are the GCaMPs and their derivatives. Current efforts in GECI development have focused on tuning them for specific applications and optical properties, such as targeting to specific cellular compartments and color. A regularly updated overview of GECIs, along with some of their key specifications, can be found at OpenOptogenetics (http://openoptogenetics.org).

Genetically encoded voltage indicators

Compared with GECIs, GEVIs have one major disadvantage and several advantages. Their major disadvantage is the low SNR that optical voltage imaging generally achieves (this is true for both low-molecular-weight classic voltage-sensitive dyes and GEVIs). Part of the SNR problem arises from the fast sampling rate employed in voltage imaging, but even for the best voltage indicators, changes in fluorescence associated with action potentials are also small when compared with calcium indicators. The main advantages of voltage indicators are their responsiveness to subthreshold activities (including membrane hyperpolarization) and their ability to resolve higher signal frequencies. Voltage imaging can provide information about both the input (synaptic potentials) and the output (action potentials) of neurons, and hence, offers access to neuronal computation rather than to coding (representations) only.

© 2013 Knöpfel

NOTES

The first prototypical GEVI was reported in 1997, the same year as the first GECIs, although getting GEVIs to satisfactorily function in mammalian neurons took another 10 years (reviewed in Mutoh et al., 2012). The currently prevalent design principle of FP-based GEVIs is based on the use of isolated voltage-sensing domains derived from voltage-sensitive membrane proteins, with FPs providing a readout of their voltage-dependent conformational state. This class of GEVIs has been given the acronym VSFP (voltage-sensitive fluorescent protein). The voltage-sensing domain used to generate the first series of VSFPs (VSFP1) was derived from a potassium channel (Kv2.1). However, like other early GEVIs, this engineered protein was not efficiently targeted to the plasma membrane, resulting in excessive background fluorescence and, consequently, a poor SNR. The first GEVI that performed well in neurons was based on the voltage-sensor scaffold of the sea squirt *Ciona intestinalis* voltage sensor-containing phosphatase (Ci-VSP). The advantage of this *Ciona intestinalis*–derived scaffold is that it naturally occurs as a monomeric, self-contained domain, in contrast to the voltage-sensing domains of potassium-channel subunits that evolved in the form of tetramers. This is probably the main reason why VSFPs based on the Ci-VSP voltage-sensing domain can efficiently target the plasma membrane of mammalian cells, including neurons.

During the intervening years, several Ci-VSP-based VSFP design variants have been explored. The first involved a tandem FRET pair of FPs fused to the end of the S4 transmembrane segment of Ci-VSP. Since this design evolved from the potassium channel–based VSFP1 indicator, this family of GEVIs was named the VSFP2s. The improved variant VSFP2.3 was the first FRET-based GEVI to enable optical imaging of spontaneous action and synaptic potentials in neurons.

Members of the VSFP2 family differ with regard to the FPs used. Whereas the best-tuned versions for each color variant differ only modestly in sensitivity and kinetic parameters when compared in cultured PC12 cells, the species of FPs used has a dramatic impact on membrane-targeting efficiency and effective signal amplitude when used in mammalian neurons. In the latest FRET-based VSFP design, the voltage-sensing domain is sandwiched between two FPs. We termed this family "VSFP-butterflies," which probably represents the best-performing probes for monitoring subthreshold membrane oscillations *in vivo*.

Other classes of VSFPs have been developed that use a single FP instead of a pair. This family of the VSFP class of voltage indicators contains members that span the FP color spectrum—from cyan to far red—and includes the green fluorescent VSFP-ArcLight variants. Monochromatic VSFP variants have also been designed to incorporate circularly permuted fluorescent proteins (cpFPs), but these have yet to match the success achieved with cpFP-based calcium indicator proteins.

A totally different class of GEVIs is based on microbial opsins used in a reverse mode, that is, exploiting voltage-induced light signals instead of the regular light-induced voltage signal. The current limitations of these opsin-based voltage indicators are their low-fluorescence quantum yield (resulting in low brightness relative to normal tissue fluorescence) and their low effective excitability using 2P fluorescence excitation. This is probably why fluorescence related to Arch (a microbial light-driven proton pump, Archeorhodopsin-3) remained virtually undetectable when enhanced GFP (eGFP)–tagged Arch was expressed in the cortex of living mice, whereas fluorescence of the eGFP tag and of VSFP2.3 was readily detected in control mice and greatly exceeded autofluorescence under the same experimental conditions (Mutoh et al., 2012). A recent report indicated that increasing excitation intensities to very high levels can induce a more than proportional increase in Arch fluorescence intensity (Maclaurin et al., 2013). Whether this effect can raise opsin-based GEVIs to a performance level that makes them suitable for *in vivo* imaging is an open question. (A regularly updated overview of GEVIs, along with some of their key specifications, is available at http://openoptogenetics.org.)

Large-scale recordings of neuronal activities using optogenetic activity indicators

Optogenetic (genetically encoded) indicators allow the imaging of very large numbers of neurons, while cell class–specific targeting of the indicators minimizes the loss of information that would otherwise result by averaging these data over heterogeneous cell populations. In principle, several cell classes (e.g., excitatory and inhibitory cells) might be monitored simultaneously, using indicators of different colors, with high spatial and temporal resolution. Moreover, GECIs facilitate making chronic recordings: sampling data over multiple sessions spaced out by days or weeks. This not only enables the investigation of

© 2013 Knöpfel

NOTES

slowly developing, experience-dependent changes in activity patterns that may be related to behavioral changes, but also increases the number of cells that can be sampled in high-resolution experiments from a single animal.

For the initial exploration of these ideas, we generated transgenic mice that express the GECI GCaMP2 under the cell class–specific regulatory sequences of the potassium channel Kv3.1. These mice allowed us to image presynaptic calcium transients in en passant synapses formed between cerebellar granule cells and Purkinje neurons and postsynaptic calcium transients in the olfactory bulb glomeruli of living mice (Díez-García et al., 2005; Fletcher et al., 2009).

The principles of GEVI-based *in vivo* circuit imaging were first demonstrated by monitoring sensory-evoked responses from layer 2/3 pyramidal cells. Newer red-shifted VSFPs (e.g., VSFP-Butterfly 1.2) exhibit markedly enhanced localization to neuronal membranes after long-term expression *in vivo* as well as giving a large-amplitude voltage report (reviewed in Mutoh et al., 2003; Knöpfel, 2012). VSFP-Butterfly 1.2 resolves action potentials from individual neurons in single sweeps and enables the imaging of subthreshold membrane oscillations *in vivo*.

Imaging very large pools of genetically specified classes of neurons reveals their synchronized and coordinated activities. The example shown in Figure 1 illustrates how the high spatial and temporal resolution of VSFP-based voltage imaging allows us to study the temporal organization of activities in multiple cortical areas responding to sensory inputs and their initiation of motor programs. Transgenic mice that express VSFP-Butterfly 1.2 (and a newer variant with a faster chimeric voltage sensor domain) have already been generated, and we expect to present initial results obtained using these mice during the Short Course presentation.

Acknowledgments

I thank all members of my lab for their dedication to the ideas summarized in this chapter over the last 15 years. Work in my lab has been supported by intramural grants from RIKEN, the Japanese Society for the Promotion of Science, the Human Frontiers Science Program, the National Institutes of Health, the Canadian Institutes of Health Research, and the Ministry of Education, Culture, Sports, Science and Technology of Japan. Portions of this chapter have been excerpted and paraphrased from the published reviews from my lab listed below. References are given in the text sparsely and essentially only if not found in these extensively referenced reviews.

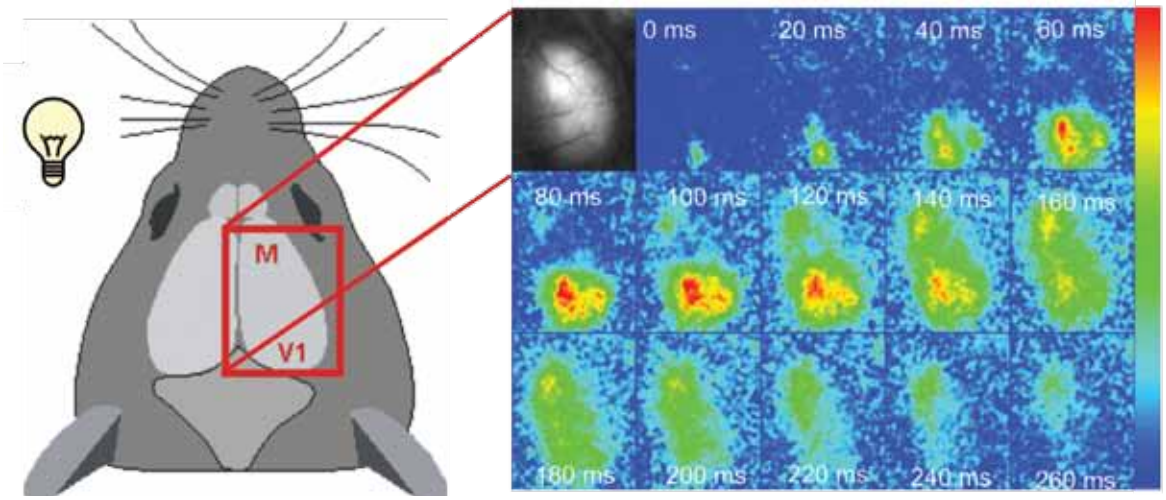

Figure 1. Voltage imaging in living mice. Spread of neuronal information from sensory to motor areas. Left: VSFP-Butterfly 1.2 was expressed over a large cortical area, including motor cortex (M) and primary visual cortex (V1). A flash of light at *t* = 0 ms triggered a response in V1 and higher visual areas, from which it spread over the hemisphere, evoking a response in the motor cortex.

© 2013 Knöpfel

NOTES

References

Alford SC, Wu J, Zhao Y, Campbell RE, Knöpfel T (2013) Optogenetic reporters. Biol Cell 105:14–29.

Díez-García J, Matsushita S, Mutoh H, Nakai J, Ohkura M, Yokoyama J, Dimitrov D, Knöpfel T. (2005) Activation of cerebellar parallel fibers monitored in transgenic mice expressing a fluorescent Ca^{2+} indicator protein. Eur J Neurosci. 22:627-635.

Dugué GP, Akemann W, Knöpfel T (2012) A comprehensive concept of optogenetics. Prog Brain Res 196:1–28.

Fletcher ML, Masurkar AV, Xing J, Imamura F, Xiong W, Nagayama S, Mutoh H, Greer CA, Knöpfel T, Chen WR. (2009) Optical imaging of postsynaptic odor representation in the glomerular layer of the mouse olfactory bulb. J Neurophysiol. 102:817-830.

Insel TR, Landis SC, Collins FS (2013) Research priorities. The NIH BRAIN Initiative. Science 340:687–688.

Knöpfel T (2012) Genetically encoded optical indicators for the analysis of neuronal circuits. Nat Rev Neurosci 13:687–700.

Knöpfel T, Díez-García J, Akemann W (2006) Optical probing of neuronal circuit dynamics: genetically encoded versus classical fluorescent sensors. Trends Neurosci 29:160–166.

Maclaurin D, Venkatachalam V, Lee H, Cohen AE (2013) Mechanism of voltage-sensitive fluorescence in a microbial rhodopsin. Proc Natl Acad Sci USA 110:5939–5944.

Mutoh H, Knöpfel T (2013) Probing neuronal activities with genetically encoded optical indicators: from a historical to a forward-looking perspective. Pflugers Arch 465:361–371.

Mutoh H, Akemann W, Knöpfel T (2012) Genetically engineered fluorescent voltage reporters. ACS Chem Neurosci 3:585–592.

Sherrington C (1940) Man on his nature. Cambridge, UK: Cambridge UP.

© 2013 Knöpfel